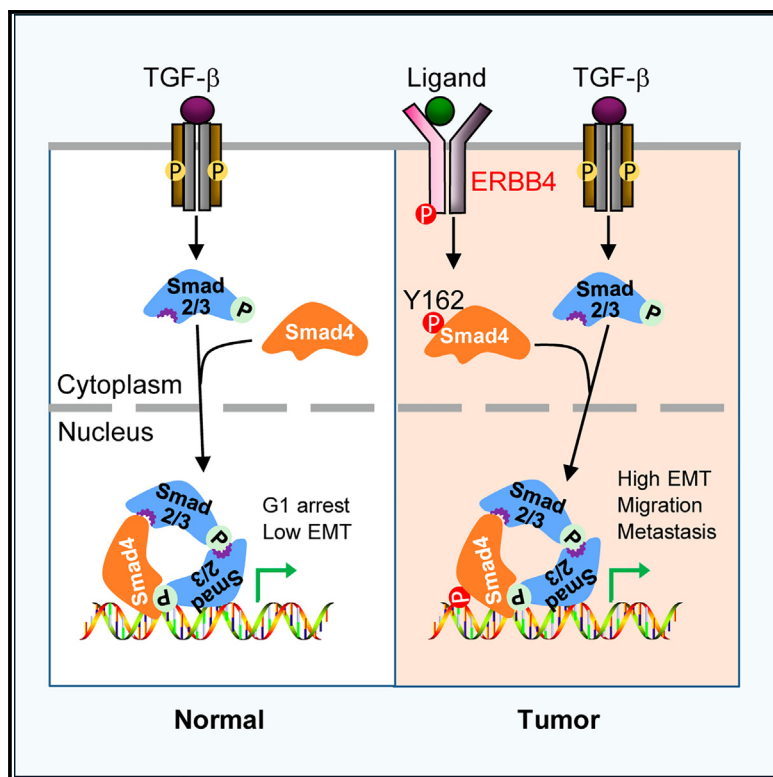


ERBB4 selectively amplifies TGF- β pro-metastatic responses

Graphical abstract



Authors

Peihong Luo, Huanyu Hong,
Baoling Zhang, ..., Xia Lin, Yi Yu,
Xin-Hua Feng

Correspondence

yuyi_lsi@zju.edu.cn (Y.Y.),
fenglab@zju.edu.cn (X.-H.F.)

In brief

Peihong Luo et al. describe in this paper that ERBB4 phosphorylates SMAD4 to mediate a select set of TGF- β transcriptional responses, which underscores the importance of SMAD4 tyrosine phosphorylation. Animal model data suggest that SMAD4 tyrosine phosphorylation promotes cell migration and tumor metastasis.

Highlights

- TGF- β inhibits cell proliferation and paradoxically promotes metastasis
- ERBB4 selectively boosts TGF- β metastasis-promoting responses
- ERBB4 phosphorylates SMAD4 Tyr-162 to enable SMAD4 occupancy on the EMT gene promoters
- Tyr-162 phosphorylation drives TGF- β migratory responses and tumor metastasis



Article

ERBB4 selectively amplifies TGF- β pro-metastatic responses

Peihong Luo,^{1,2,3} Huanyu Hong,^{1,2,3} Baoling Zhang,^{1,2,3} Jie Li,^{1,2,3} Shuyi Zhang,^{1,2,3} Chaomin Yue,¹ Jin Cao,^{1,2,3} Jia Wang,^{1,2,3} Yuhan Dai,^{1,2,3} Qingqing Liao,¹ Pinglong Xu,^{1,3} Bing Yang,^{1,3} Xia Liu,⁴ Xia Lin,⁵ Yi Yu,^{1,2,3,*} and Xin-Hua Feng^{1,2,3,6,7,*}

¹MOE Key Laboratory of Biosystems Homeostasis & Protection, and Zhejiang Provincial Key Laboratory of Cancer Molecular Cell Biology, Life Sciences Institute, Zhejiang University, Hangzhou, Zhejiang 310058, China

²Center for Life Sciences, Shaoxing Institute, Zhejiang University, Shaoxing, Zhejiang 321000, China

³Cancer Center, Zhejiang University, Hangzhou, Zhejiang 310058, China

⁴ZJU-Hangzhou Global Scientific and Technological Innovation Center, Zhejiang University, Hangzhou, Zhejiang 311215, China

⁵Department of Hepatobiliary and Pancreatic Surgery and Zhejiang Provincial Key Laboratory of Pancreatic Disease, The First Affiliated Hospital, Zhejiang University School of Medicine, Hangzhou, Zhejiang 310003, China

⁶The Second Affiliated Hospital, Zhejiang University, Hangzhou, Zhejiang 310009, China

⁷Lead contact

*Correspondence: yuyi_lsi@zju.edu.cn (Y.Y.), fenglab@zju.edu.cn (X.-H.F.)

<https://doi.org/10.1016/j.celrep.2024.115210>

SUMMARY

Transforming growth factor β (TGF- β) is well known to play paradoxical roles in tumorigenesis as it has both growth-inhibitory and pro-metastatic effects. However, the underlying mechanisms of how TGF- β drives the opposing responses remain largely unknown. Here, we report that ERBB4, a member of the ERBB receptor tyrosine kinase family, specifically promotes TGF- β 's metastatic response but not its anti-growth response. ERBB4 directly phosphorylates Tyr162 in the linker region of SMAD4, which enables SMAD4 to achieve a higher DNA-binding ability and potentiates TGF- β -induced gene transcription associated with epithelial-to-mesenchymal transition (EMT), cell migration, and invasion without affecting the genes involved in growth inhibition. These selective effects facilitate lung cancer metastasis in mouse models. This discovery sheds light on the previously unrecognized role of SMAD4 as a substrate of ERBB4 and highlights the selective involvement of the ERBB4-SMAD4 regulatory axis in tumor metastasis.

INTRODUCTION

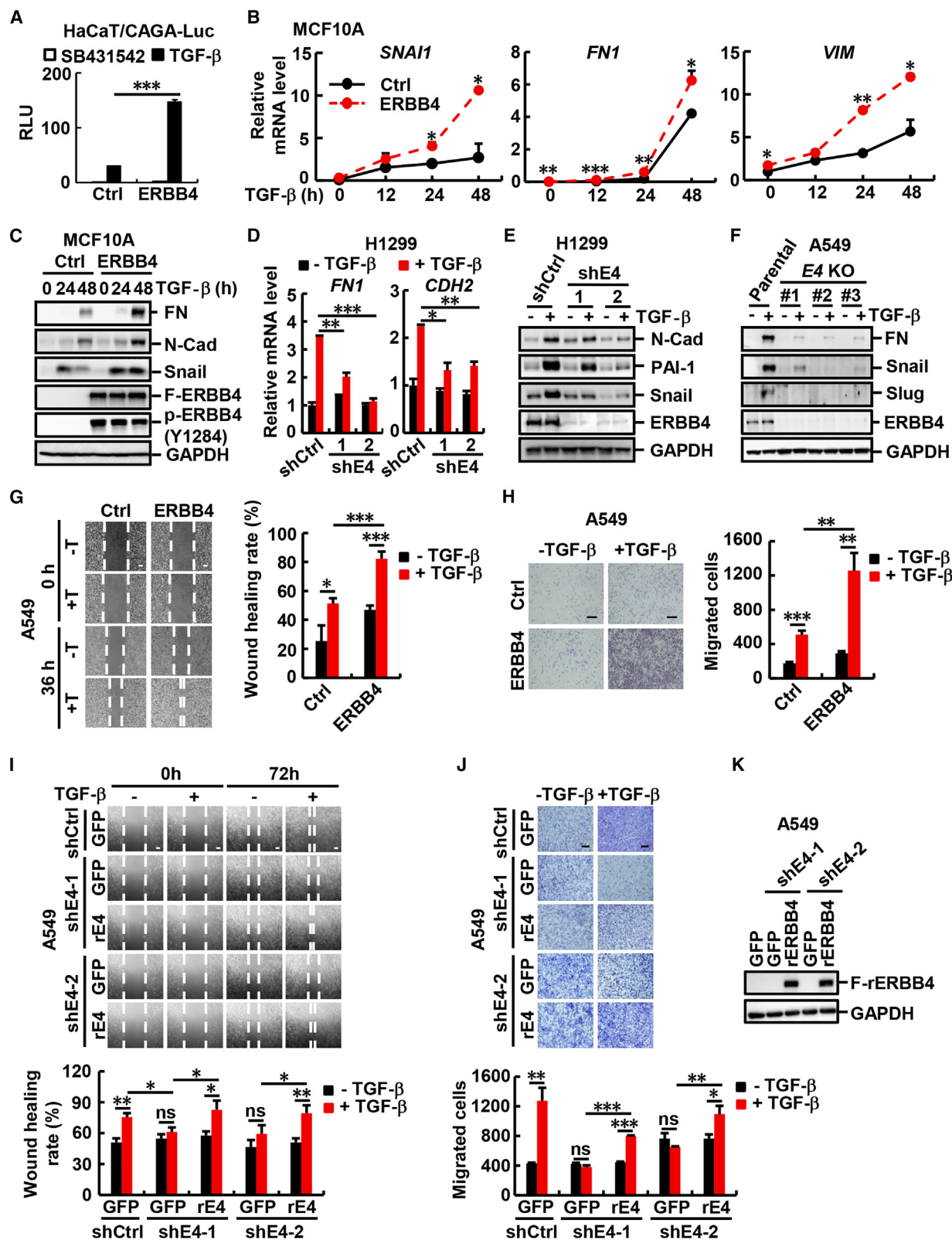
Our comprehension of oncogenes, tumor suppressors, and crucial signaling pathways in cancer initiation and advancement has progressed significantly in tumor biology. Notable examples include the transforming growth factor β (TGF- β) signaling pathway and the epidermal growth factor receptor (EGFR) family of receptor tyrosine kinases (RTKs; ERBB), which have been established as significant factors in the development of various human cancers. While the ERBB family, comprising four members—EGFR (also known as ERBB1), ERBB2 (HER2), ERBB3, and ERBB4—has been extensively studied for their oncogenic properties, it is well established that TGF- β has a dual role in cancer. TGF- β can suppress tumor initiation and development while also promoting effects that lead to tumor metastasis. Yet, the specific mechanisms through which TGF- β elicits these opposing responses are not fully understood.

The epithelial-to-mesenchymal transition (EMT) is recognized as a crucial process facilitating the invasion and metastasis of carcinomas during the progression of cancer. EMT encompasses the phenomenon where epithelial cells undergo changes, losing their cell polarity and intercellular adhesion while transitioning into mesenchymal cells. Specifically, the activity of

the TGF- β is a prominent instigator of EMT.^{1–4} TGF- β signals are transmitted through its cell surface receptors, inducing the phosphorylation and subsequent activation of downstream mediators, SMAD2 and SMAD3.^{5–9} The phosphorylated SMAD2/3 molecules then form a transcriptional activator complex in conjunction with SMAD4 and other transcription factors, thereby regulating the transcription of TGF- β target genes.¹⁰ Throughout the process of EMT, the SMAD complex can interact with Snail and Zeb1/2 to govern the transcription of genes related to EMT, ultimately leading to the downregulation of epithelial marker genes and the upregulation of mesenchymal marker genes.^{4,8,11–14}

It is widely documented that oncogenic and tumor-suppressor pathways are intricately connected. The complex interactions between oncogenes and tumor-suppressor genes highlight the intricate nature of cancer biology and provide valuable insights for potential therapeutic interventions. Indeed, TGF- β frequently collaborates with other signaling pathways, such as the RTK pathway, to instigate a complete EMT.¹⁵ The interaction between TGF- β signaling and RTK signaling pathways can be varied, involving cooperation or mutual antagonism. In normal tissues or during the early stages of tumor development, TGF- β serves as a potent growth suppressor, while RTKs are often





(legend on next page)

implicated in promoting cell growth, and both pathways can counteract each other's cellular growth functions.¹⁶ However, as tumors progress, TGF- β can impact epithelial plasticity and cell motility, leading to EMT, which contributes to tumor metastasis.^{2,11,14,17–19} Furthermore, there is an established link between ERBB family members and TGF- β signaling during EMT at various regulatory levels. TGF- β can transactivate EGFR and stimulate the production of EGFR ligand heparin-binding (HB)-EGF, thus promoting cancer cell migration and invasion through the PI3K/Akt, ERK, and p38 MAPK signaling pathways,^{14,20,21} Additionally, the activation of HER2/EGFR induces nuclear accumulation of SMAD3 by phosphorylating SMAD3 at Ser208 via AKT, leading to the expression of genes related to EMT and cell migration.²² Similarly, heregulin (HRG)- β 1/ERBB3 induces EMT, cancer cell migration, and invasion through the PI3K/Akt-phospho-SMAD2-Snail signaling pathway.²³ Recent studies have also indicated increased expression of ERBB4 and pERBB4 in podocytes after TGF- β 1 treatment, suggesting a potential association between ERBB4 and the TGF- β signaling pathway.²⁴ Yet, the interaction between TGF- β and ERBB signaling pathways in regulating cancer progression is, thus far, not completely understood.

Our current study illustrates the role of ERBB4 as a SMAD4 kinase, directly phosphorylating SMAD4 at Tyr162. The tyrosine-phosphorylated SMAD4 exhibits increased binding activity to chromatin and leads to enhanced expression of EMT genes upon TGF- β stimulation, consequently promoting cell mobility and facilitating lung cancer metastasis. Hence, our findings offer an explanation for how TGF- β signaling is switched from being growth inhibitory to pro-metastatic and also shed light on a distinctive mechanism governing the interaction between TGF- β signaling and RTK signaling in metastasis.

RESULTS

ERBB4 potentiates TGF- β -mediated EMT and migratory responses

Our initial screen for SMAD-interacting proteins revealed ERBB4 as a potential binding partner of SMAD4 (data not shown). Given the known connections of TGF- β and ERBB4

to tumor development and progression, we are intrigued by the potential implications of the interaction between SMAD4 and ERBB4 in cancer. To explore this further, we first examined the impact of ERBB4 on TGF- β -induced transcriptional responses. Our findings indicated that ectopic expression of ERBB4 significantly enhanced TGF- β -mediated transcriptional activation using two synthetic TGF- β -responsive reporters, CAGA-luc (Figure 1A) and SMAD-binding element (SBE)-luc (Figure S1A), in immortalized human keratinocyte HaCaT cells. Moreover, stable expression of ERBB4 in human mammary epithelial MCF10A cells substantially increased the transcription of EMT-related genes, including *SNAI1*, *FN1*, *VIM* (Figure 1B), and *SERPINE1* (Figure S1B). Correspondingly, ERBB4 also elevated the protein levels of fibronectin (FN), N-cadherin (N-Cad), and Snail induced by TGF- β (Figure 1C). Similar effects of ERBB4 were also observed in human non-small cell lung cancer (NSCLC) A549 cells (Figures S1C–S1E). Conversely, silencing ERBB4 with short hairpin RNA (shRNA) led to decreased mRNA and protein levels of *FN1*, *CDH2*, *SERPINE1*, *SNAI1*, and *SNAI2* in human NSCLC cells, including H1299 (Figures 1D, 1E, and S1F), Calu-3 (Figure S1G), and SPC-A-1 (Figure S1H). Additionally, CRISPR-Cas9-directed knockout (KO) of ERBB4 using three different small guide RNAs (sgRNAs) resulted in a significant decrease in the expression of EMT markers induced by TGF- β in A549 cells (Figure 1F). Taken together, these results indicated that ERBB4 positively regulates the expression of EMT marker genes induced by TGF- β .

Since EMT represents a cellular process from polarized epithelial cells to motile and invasive mesenchymal cells, we next examined whether ERBB4 modulated TGF- β -regulated cell migration and invasion. As shown in Figures 1G and 1H, TGF- β markedly increased the tumor migration of A549 cells, which was further accelerated by ERBB4, as determined by both wound-healing and transwell assays. Similar results were also observed in MCF10A cells (data not shown). Conversely, shRNA- or sgRNA-mediated ERBB4 depletion attenuated the TGF- β effects in A549 (Figures 1I, 1J, S2A, and S2B), H1299 (Figure S2C), and SPC-A-1 cells (Figures S2D and S2E). Importantly, RNAi-resistant ERBB4 (rERBB4)

Figure 1. ERBB4 promotes TGF- β -induced EMT

- (A) HaCaT cells were transfected with expression plasmids of CAGA-luc, Renilla-luc, and ERBB4 and treated with TGF- β (2 ng/mL) for 8 h. Relative luciferase activities were measured as described in the STAR Methods.
- (B) MCF10A cells stably expressing FLAG-ERBB4 were treated with TGF- β (2 ng/mL) for the indicated time periods and subjected to RT-qPCR.
- (C) MCF10A cells stably expressing ERBB4 were stimulated with TGF- β (2 ng/mL) for 24 or 48 h. Cells were harvested and blotted with the indicated antibodies.
- (D) H1299 cells with ERBB4 knockdown were treated with TGF- β (2 ng/mL) for 24 h and subjected to RT-qPCR.
- (E) H1299 cells with ERBB4 knockdown were treated with TGF- β (2 ng/mL) for 48 h. Cells were harvested and blotted with the indicated antibodies.
- (F) A549 parental and ERBB4-KO cells were treated with TGF- β (2 ng/mL) for 48 h. Cells were harvested and blotted with the indicated antibodies.
- (G) Artificial wounds were created by scratching, and the cells were cultured with or without 2 ng/mL TGF- β for 36 h. Cell migration was measured by wound closure. The wound-healing rate was quantitated and statistically analyzed (right). Scale bars, 100 μ m.
- (H) A549 cells were treated with 2 ng/mL TGF- β for 24 h and allowed to migrate through the membrane in transwells. Migrated cells were stained with 1% crystal violet and photographed. Migrated cells were quantitated and statistically analyzed (right). Scale bars, 100 μ m.
- (I and J) A549 cells expressing a control shRNA or ERBB4 shRNAs were rescued with GFP or shRNA-resistant ERBB4 (rERBB4). Cells were cultured with or without 2 ng/mL TGF- β for 72 h, and cell migration was determined by wound-healing assay (I) and transwell assay (J) as described in (G) and (H), respectively. The quantitation was done similarly as described in (G) and (H), respectively. Scale bars, 100 μ m.
- (K) The levels of FLAG-rERBB4 were determined by western blotting with anti-FLAG antibody.

For all plots, data are shown as mean \pm SEM; $n = 3$. Statistical analysis was performed using a two-tailed Student's t test. * $p < 0.05$, ** $p < 0.01$, and *** $p < 0.001$. ns, non-significant.

See also Figure S1 and S2.

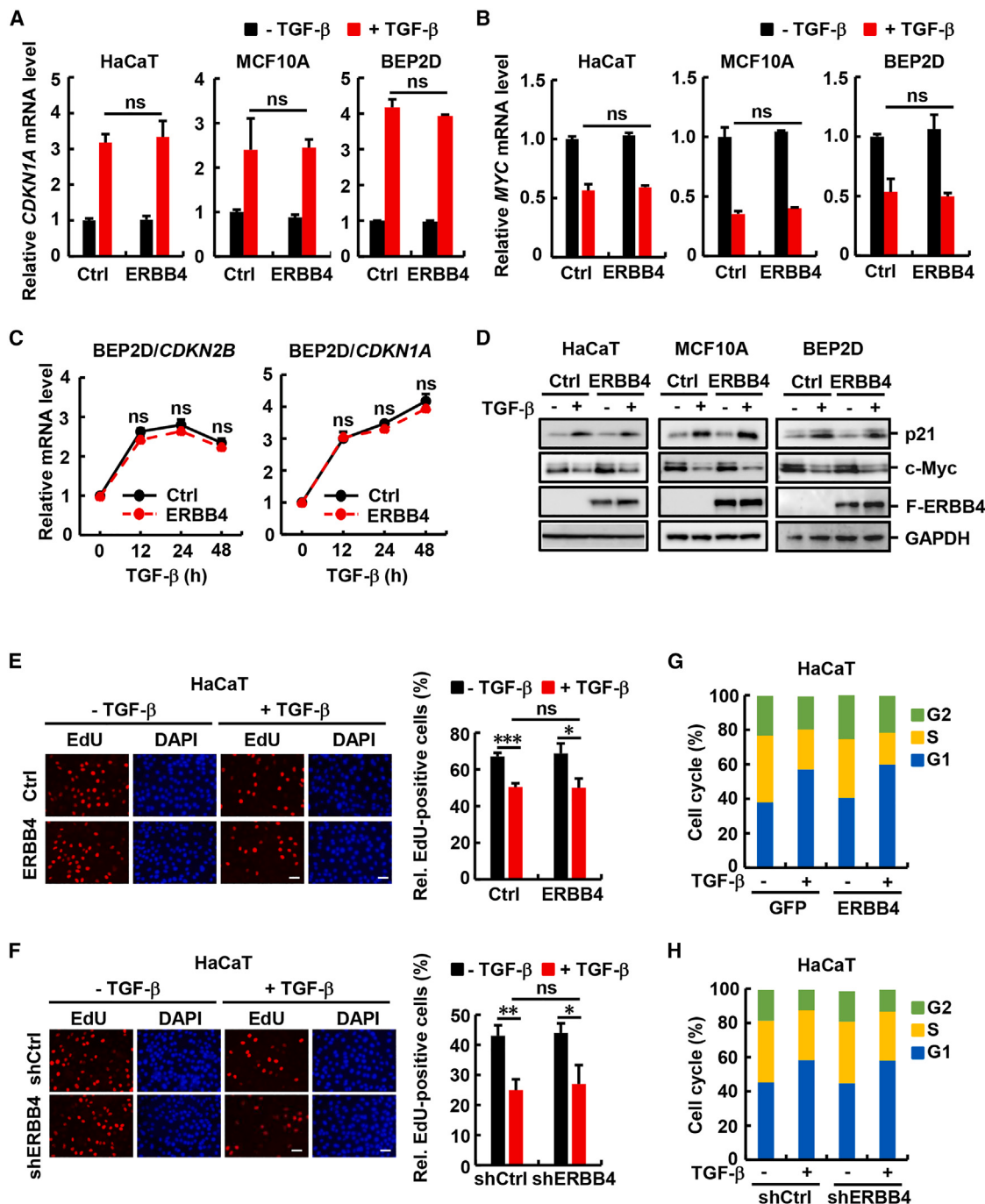


Figure 2. ERBB4 has no effects on TGF- β -induced growth inhibitory responses

(A and B) HaCaT, MCF10A, and BEP2D cells stably expressing FLAG-ERBB4 were treated with TGF- β (2 ng/mL) for 12 h. Total mRNAs were isolated and analyzed by RT-qPCR using primers specific to *CDKN1A* (A) or *MYC* (B).

(C) BEP2D cells stably expressing FLAG-ERBB4 were treated with TGF- β (2 ng/mL) for the indicated time periods and subjected to RT-qPCR.

(D) HaCaT, MCF10A, and BEP2D cells stably expressing ERBB4 were stimulated with TGF- β (2 ng/mL) for 24 h. Cells were harvested and blotted with the indicated antibodies.

(E) ERBB4-overexpressing and control HaCaT cells were treated with TGF- β (2 ng/mL) for 48 h. EdU incorporation was examined using an EdU staining kit, which was quantitatively analyzed (bar graph). Scale bars, 50 μ m.

(legend continued on next page)

could fully restore the migration of ERBB4-knockdown A549 cells (Figures 1I and 1J) when FLAG-rERBB4 was re-expressed in shERBB4 cells (Figure 1K).

ERBB4 does not impact TGF- β growth-inhibitory responses

TGF- β exhibits two distinct responses in regulating tumors. It primarily causes G1 arrest in epithelial cells by upregulating the transcription of cyclin-dependent kinase (CDK) inhibitors and reducing c-Myc expression. Our investigation aimed to determine whether ERBB4 generally enhances the transcriptional responses of TGF- β or is specifically limited to promoting EMT responses. In this study, we evaluated the impact of ERBB4 on the mRNA levels of *CDKN1A* (encoding p21) and *MYC* in normal epithelial cells. Although ERBB4 had a notable effect on EMT genes (Figures 1, S1, and S2), it did not further enhance *CDKN1A* expression in HaCaT, MCF10A, or BEP2D cells (Figure 2A). Similarly, ERBB4 did not modify the TGF- β -mediated downregulation of *MYC* in these cell lines (Figure 2B). Additionally, the ectopic expression of ERBB4 did not interfere with the time-dependent regulation of *CDKN2B* (encoding p15) and *CDKN1A* in response to TGF- β (Figure 2C). The upregulation of p21 protein levels and the downregulation of c-Myc protein levels in response to TGF- β align with the observed changes at the mRNA levels (Figure 2D).

To establish a link between ERBB4's impact on molecular changes and its influence on the cell cycle status, we analyzed TGF- β -induced G1 arrest using EdU staining and flow cytometric assays. As anticipated, TGF- β resulted in a significant decrease in EdU staining (Figures 2E, 2F, and S3) and an increase in G1 content (Figures 2G and 2H). Importantly, the overexpression or knockdown of ERBB4 did not affect TGF- β -mediated inhibition on DNA synthesis in HaCaT cells (Figures 2E–2H) or in BEP2D and MCF10A cells (Figures S3A–S3C). Overall, these findings indicate that ERBB4 specifically enhances EMT responses without impacting the growth-inhibitory responses of TGF- β .

ERBB4 kinase activity is essential for regulating TGF- β -induced EMT

Since ERBB4 is a protein tyrosine kinase, we were wondering if the kinase activity of ERBB4 is required for its regulation of TGF- β -induced EMT. To test this, we first employed small-molecule inhibitors of the ERBB4 kinase: poziotinib, afatinib, and AST-1306.^{25–27} These inhibitors could abolish the effect of ERBB4 on TGF- β -induced gene expression and cell migration in MCF10A cells (Figures 3A and 3B). In addition, the kinase-dead ERBB4 mutant with lysine 751 substituted with methionine (K751M) failed to enhance TGF- β -induced expression of mesenchymal markers and cell migration in MCF10A (Figures 3A and 3B) and A549 cells (Figures S4A and S4B).

(F) ERBB4-knockdown and control HaCaT cells were treated with TGF- β (2 ng/mL) for 48 h. EdU incorporation was examined using an EdU staining kit, which was quantitatively analyzed (bar graph). Scale bars, 50 μ m.

(G and H) ERBB4-overexpressing (G) or -knockdown (H) HaCaT cells were treated with TGF- β (2 ng/mL) for 48 h. The cell cycle was analyzed using flow cytometry.

For all plots, data are shown as mean \pm SEM; $n = 3$. Statistical analysis was performed using a two-tailed Student's t test. * $p < 0.05$, ** $p < 0.01$, and *** $p < 0.001$. ns, non-significant.

See also Figure S3.

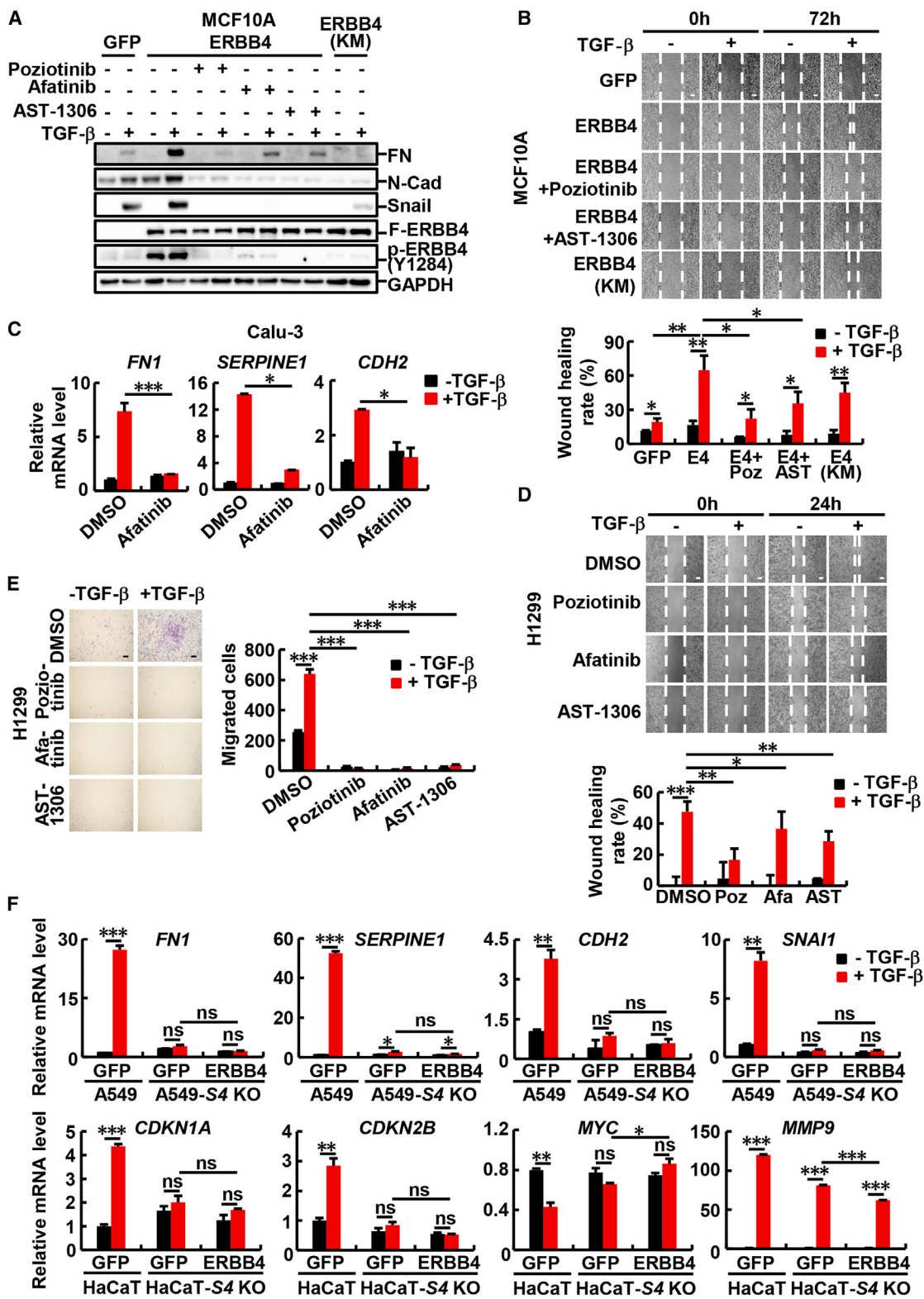
We next examined the effect of ERBB4 inhibition on TGF- β -induced EMT in several NSCLC cell lines, which express high levels of endogenous ERBB4. Whereas TGF- β profoundly induced the transcription of *FN1*, *SERPINE1*, and *CDH2* genes, treatment of the ERBB4 inhibitor afatinib completely or almost completely diminished these TGF- β -induced responses in Calu-3 (Figure 3C) and SPC-A-1 cells (Figure S4C). Similar results were obtained with poziotinib, afatinib, or AST-1306 treatment in H1299 (Figures 3D and 3E) and SPC-A-1 cells (Figures S4D and S4E), demonstrating the essential role of the tyrosine kinase activity of ERBB4 in promoting TGF- β -induced EMT and migratory responses.

ERBB4 amplifies EMT independent of SMAD4

In advanced tumors, TGF- β promotes tumor progression by inducing EMT through a combination of SMAD-dependent and -independent mechanisms. While the SMAD molecules are critical for EMT, non-SMAD signaling mediators such as ERK and PI3K-AKT, which are downstream mediators of ERBB4, also contribute to TGF- β -induced EMT.^{14,28–30} Hence, we determined whether ERBB4 upregulates TGF- β responses in the absence of canonical SMAD signaling by knocking out the *SMAD4* gene in A549 cells. RT-qPCR and western blotting analyses showed that the ablation of SMAD4 abolished TGF- β -induced upregulation of *FN1*, *SERPINE1*, *CDH2*, and *SNAI1* (Figure 3F) and their respective proteins (Figure S4F), indicating the indispensable role of SMAD4 in TGF- β -induced EMT in NSCLC cells. Importantly, ERBB4 failed to enhance TGF- β -induced expression of these mesenchymal markers in *SMAD4*^{−/−} cells (Figure 3F, top row, and S4F), demonstrating that ERBB4 upregulates TGF- β -induced EMT through canonical SMAD signaling. In addition, TGF- β -induced growth-inhibitory gene responses also depended on SMAD4, as indicated by the lack of *CDKN1A* and *CDKN2B* upregulation and *MYC* downregulation in *SMAD4*-KO cells (Figure 3F, bottom left/middle). Notably, we found that TGF- β -induced *MMP9* transcription was independent of SMAD4, and ERBB4 expression had no or little inhibitory effect on TGF- β -induced *MMP9* transcription (Figure 3F, bottom right).

ERBB4 directly interacts with and phosphorylates SMAD4 on Tyr162

To elucidate the precise mechanism by which ERBB4 regulates canonical TGF- β signaling, we examined the effect of ERBB4 on TGF- β signal transduction, from SMAD2/3-activating phosphorylation and SMAD2/3-SMAD4 complex formation and nucleocytoplasmic shuttling of SMAD4 to the DNA-binding and transactivation activity of SMAD4. Our results showed that the stable expression of ERBB4 did not affect the TGF- β -induced SMAD2 and SMAD3 phosphorylation, as well as the SMAD complex



(legend on next page)

formation and nuclear translocation in MCF10A cells (data not shown).

To verify whether ERBB4 is a SMAD4-associated protein as indicated in the initial antibody array-based screen (data not shown), we examined the colocalization and direct interaction between SMAD4 and ERBB4. ERBB4 and SMAD4 were found to colocalize in the cytoplasm, which, however, did not require TGF- β stimulation (Figure S5A). Notably, co-immunoprecipitation (co-IP) experiments further confirmed the physiological interaction between endogenous ERBB4 and SMAD4 (Figure 4A). Furthermore, direct *in vitro* binding assays found that purified recombinant glutathione S-transferase (GST)-SMAD4 protein could bind to the *in-vitro*-translated FLAG-tagged ERBB4 intracellular domain (4ICD). Specifically, as shown in Figure 4B, GST-tagged SMAD4 protein, but not GFP protein, could bind to the 4ICD, indicating a direct binding of SMAD4 to the cytoplasmic domain of ERBB4. Furthermore, the MH2 domain, but not the MH1 or linker domain, in SMAD4 mediated this binding (Figure S5B).

Due to ERBB4's tyrosine kinase activity, we investigated its ability to phosphorylate SMAD4 *in vivo* and *in vitro*. In transfected HEK293T cells, overexpressed ERBB4 markedly phosphorylated SMAD4 (Figure 4C), while the kinase-dead ERBB4 (K751M) mutant failed to induce phosphorylation, as determined by western blotting using the phospho-tyrosine-specific antibody PY100 (Figure 4C). An *in vitro* kinase assay showed that *in-vitro*-translated ERBB4, but not ERBB4 (K751M), effectively phosphorylated recombinant GST-SMAD4 proteins (Figure 4D), supporting the direct tyrosine phosphorylation of SMAD4 by ERBB4.

In the pursuit of identifying the phosphorylation sites on SMAD4, we conducted a series of experiments involving the generation of various deletion mutants of SMAD4. Our observations indicated that ERBB4 could effectively phosphorylate the full-length SMAD4 or mutants containing the linker region, such as MH1-linker (NL) and linker-MH2 (LC) regions, but not the MH1+MH2 (NC) domain of SMAD4 (Figures S5C and 4E). This suggests that ERBB4 targets the linker region of SMAD4. Subsequent mass spectrometry analysis identified tyrosine residues 114 (Tyr 114 or Y114), Y117, Y162, Y353, Y412, and Y513 as potential phosphorylation sites (Figure S5D). We then engineered unphosphorylatable SMAD4 mutants by substituting

these sites with phenylalanine (Y-to-F mutation). Notably, only the Y117F and Y162F mutants displayed significant impairment of ERBB4-induced phosphorylation of SMAD4 (Figure S5E), demonstrating Y117 and Y162 as ERBB4-induced phosphorylation sites. We subsequently investigated the impact of these phosphorylation sites on ERBB4-regulated SMAD4 activity by generating Y-to-E (tyrosine-to-glutamic acid) mutants and assessing their effects on the TGF- β -induced CAGA-luc response in SMAD4-KO A549 cells. Our results indicated that, while wild-type SMAD4 restored TGF- β -induced CAGA-luc reporter activity in SMAD4-null cells, the Y162E mutant exhibited a stronger effect, suggesting that Y162 represents the primary phosphorylation site of SMAD4 induced by ERBB4 (Figure S5F).

Subsequently, we generated a phospho-specific polyclonal antibody (PY162) against the phosphorylated Y162 of SMAD4. The PY162 antibody could readily detect the phosphorylation of SMAD4 in the presence of ERBB4 but not ERBB4 (K751M) (Figure 4F). Furthermore, the PY162 antibody exhibited specificity by not recognizing the Y162 mutant while detecting the Y114F and Y117F mutants that still retained the phospho-Y162 residue (Figure 4G). It is noteworthy that PY162 successfully detected the endogenous p-SMAD4 (Y162) in A549 cells, and the stable expression of ERBB4 increased the PY162 level (Figure 4H), which could be abolished by afatinib, poziotinib, or AST-1306 treatment (Figure S5G). Although these small-molecule inhibitors can also target EGFR, we found that EGFR did not induce SMAD4 Y162 phosphorylation, indicating that the inhibitors blocked PY162 through ERBB4 (Figure S5H). Likewise, the depletion of ERBB4 with shRNA notably reduced SMAD4 Y162 phosphorylation in H1299 cells (Figure 4I). The evidence from both *in vivo* and *in vitro* experiments supports the conclusion that ERBB4 directly phosphorylates SMAD4 at Y162.

ERBB4 enhances the DNA-binding activity of SMAD4

Considering that ERBB4 directly phosphorylates SMAD4, we were intrigued about the potential regulatory role of ERBB4 on the nuclear localization and transcriptional characteristics of SMAD4 through SMAD4 phosphorylation. Initially, our investigation focused on the nuclear accumulation of SMAD4 following TGF- β stimulation. The results showed that neither ERBB4 nor ERBB4 (K751M) influenced SMAD4 nuclear accumulation in A549 cells (Figure 5A) or MCF10A cells (Figure S6A).

Figure 3. ERBB4 promotes TGF- β -induced EMT, dependent on its tyrosine kinase activity

- (A) MCF10A cells stably expressing GFP, ERBB4, or ERBB4 (K751M) were treated with the ERBB4 inhibitor poziotinib (10 μ M), afatinib (10 μ M), or AST-1306 (10 μ M) for 2 h, followed by TGF- β (2 ng/mL) treatment for 24 h or no treatment as indicated. Cells were harvested and blotted with the indicated antibodies. ERBB4 (KM), the K751M substitution mutant of ERBB4.
- (B) Cells were treated with the ERBB4 inhibitor poziotinib (10 μ M) or AST-1306 (10 μ M) and TGF- β (2 ng/mL) simultaneously for 72 h. The migration of cells was determined by wound-healing assay. The wound-healing rate was similarly quantitated and statistically analyzed as described in Figure 1G. Scale bars, 100 μ m.
- (C) Calu-3 cells were pretreated with 10 μ M afatinib for 2 h, followed by TGF- β (2 ng/mL) for 24 h or no treatment. Total mRNAs were isolated and analyzed by RT-qPCR using primers specific to *FN1*, *SERPINE1*, or *CDH2*.
- (D and E) H1299 cells were treated with a combination of TGF- β (2 ng/mL) and ERBB4 inhibitor poziotinib (10 μ M), afatinib (10 μ M), or AST-1306 (10 μ M) for 24 h. Then, a wound-healing assay (D) and transwell assay (E) were employed to determine the migration of H1299 cells. The quantitation was similarly done and statistically analyzed as described in Figure 1H, respectively. Scale bars, 100 μ m.
- (F) Parental and SMAD4-KO A549 cells were infected with the lentivirus expressing GFP or ERBB4. The mRNA levels of *FN1*, *SERPINE1*, *CDH2*, *SNAI1*, *CDKN1A*, *CDKN2B*, *MYC*, and *MMP9* were examined by RT-qPCR.
- For all plots, data are shown as mean \pm SEM; $n = 3$. Statistical analysis was performed using a two-tailed Student's t test. * $p < 0.05$, ** $p < 0.01$, and *** $p < 0.001$. ns, non-significant.

See also Figure S4.

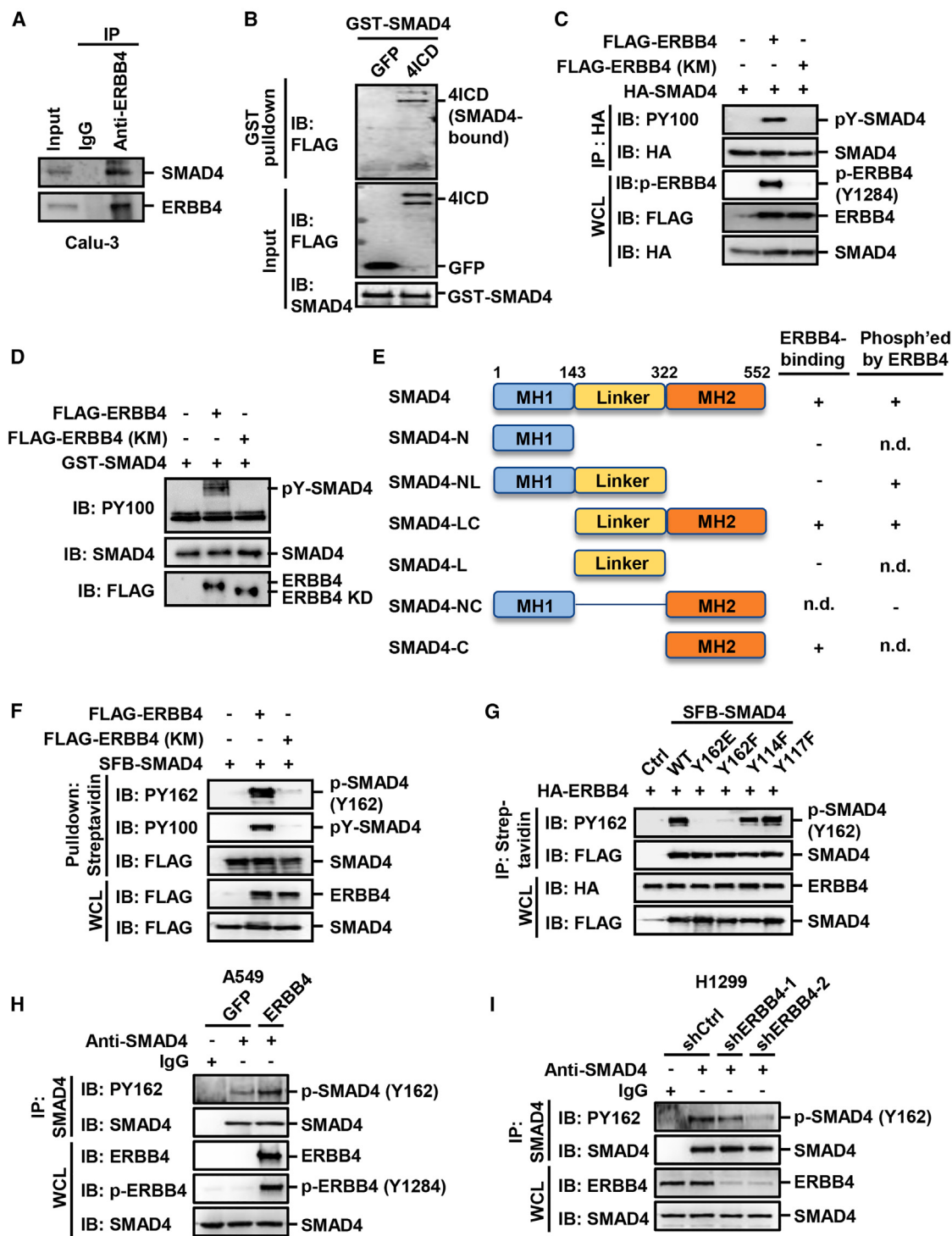


Figure 4. ERBB4 interacts with and phosphorylates SMAD4

(A) Calu-3 cells were lysed and then subjected to IP by anti-ERBB4 antibody or anti-immunoglobulin (IgG). Co-precipitated proteins were examined by western blotting with the indicated antibodies.

(B) Purified GST-SMAD4 proteins were mixed with *in-vitro*-synthesized FLAG-tagged GFP or 4ICD. GST-bound proteins and input were detected by western blotting.

(C) Plasmids encoding hemagglutinin (HA)-SMAD4 and FLAG-tagged ERBB4 or ERBB4 (K751M) were co-transfected into HEK293T cells. coIP and western blotting were carried out, and the tyrosine phosphorylation of SMAD4 was detected by the phospho-tyrosine-specific antibody PY100.

(legend continued on next page)

Furthermore, through using a heterologous GAL4-based transcription assay to assess the transactivation activity of SMAD4,³¹ no discernible disparity was observed between ERBB4 and vector expression in HaCaT cells (Figure 5B).

We subsequently evaluated the impact of ERBB4 on SMAD4's DNA-binding capability. The oligo pull-down assay showed that SMAD4 bound to the SBE oligo in response to TGF- β stimulation, and stably expressed ERBB4 in A549 cells significantly increased the TGF- β -induced SMAD4 binding to biotin-labeled SBE (Figure 5C). Conversely, the KO or knockdown of ERBB4 noticeably diminished the SBE-binding activity of SMAD4 (Figures 5D and S6B), strongly indicating that ERBB4 regulates the DNA binding of SMAD4. To confirm this effect on the native SMAD4 DNA binding, we examined the occupancy of SMAD4 on promoters of the EMT-related genes using chromatin immunoprecipitation (ChIP)-qPCR assay. Consistently, ERBB4 significantly boosted the TGF- β -induced occupancy of SMAD4 on the promoters of *SERPINE1*, *SNAI1*, and *CDH2* in A549 cells (Figure 5E), whereas the kinase-dead K751M mutant had no effect or even demonstrated a dominant-negative effect. Moreover, ERBB4 ablation substantially reduced the TGF- β -induced occupancy of SMAD4 on the promoters of these genes (Figure 5F).

SMAD4 Y162E mutant has increased binding to chromatin

To investigate the impact of Y162 phosphorylation on SMAD4's DNA-binding ability, we initially examined the direct influence of Y162 phosphorylation by introducing Y162E (mimicking phosphorylation) or Y162F (lacking phosphorylation) mutants into SMAD4-KO A549 cells. In the DNA pull-down assay, TGF- β readily induced the binding of endogenous SMAD4 to the biotin-labeled SBE oligo, which was absent in the SMAD4-KO cells (Figure 6A). The reintroduction of SMAD4 wild type or its mutants demonstrated that the Y162E mutant exhibited a higher binding to SBE than the wild type or Y162F mutant (Figure 6A). Interestingly, the Y162E mutant also enabled a higher association of SMAD2/3 with the DNA, even though the p-SMAD3 levels remained unchanged (Figure 6A). Consistent with their DNA-binding activity, expression of Y162E resulted in a greater elevation of FN and Snail protein levels compared to wild-type SMAD4 or Y162F (Figure 6B).

Further ChIP-qPCR analysis of their DNA-binding activity following TGF- β treatment revealed that, in agreement with its enhancing effect on SBE binding, the Y162E mutant showed its increased enrichment on the promoters of *SNAI1*, *CDH2*,

HAS2, and *PDGFB* (Figure 6C), as well as *SERPINE1* (Figure S6C) and *SNAI2* (Figure S6D), compared to wild-type SMAD4, while the Y162F mutant was barely detectable (Figures 6C, S6C, and S6D). Similar to the SBE binding (Figure 6A), the Y162E mutant consistently enhanced the association of SMAD2/3 on the promoters of the SMAD4 target genes (Figure 6D). In sharp contrast, the Y162E or Y162F mutant had no effect on its occupancy at the promoters of *CDKN1A* and *CKDN1C* (Figure 6E), and neither did they influence the binding of SMAD2/3 to the same promoters (Figure 6F). Overall, these findings indicate that Y162 phosphorylation of SMAD4 affects its chromatin binding capability on the EMT genes but not cyclin-dependent kinase inhibitor (CKI) genes.

SMAD4 Y162 phosphorylation facilitates the metastasis of lung cancer

We further assessed the impact of Y162 phosphorylation on TGF- β -mediated cellular responses by using SMAD4-depleted cells. In these cells, the TGF- β -induced cell migration, as measured by the wound-healing assay, was significantly reduced (Figure 7A). The reintroduction of wild-type SMAD4 rescued this effect, while the expression of Y162E resulted in a further acceleration of TGF- β -induced cell migration (Figure 7A). Moreover, compared to wild-type SMAD4 or the Y162F mutant, the expression of Y162E notably increased cell invasion (Figure 7B).

Due to the correlation between increased cell migration or invasion and augmented tumor metastasis, we investigated the metastasis-enhancing effects of ERBB4 in a mouse model. A549-luc cells expressing shCtrl or shERBB4 (shE4-1 and shE4-2) were administrated via tail vein injection into NOD/SCID (non-obese diabetic/severe combined immunodeficiency) mice. Subsequent bioluminescence imaging of live animals and hematoxylin and eosin (H&E) staining of lung sections demonstrated that mice injected with shCtrl cells developed noticeable lung tumors, whereas ERBB4 depletion notably hindered the formation of lung tumors in A549 cells, resulting in significantly fewer and smaller tumors in mice (Figures S7A–S7C). Cells expressing the kinase-dead mutant of ERBB4 (K751M) also exhibited decreased tumor formation compared to ERBB4-expressing cells (Figures 7C–7E). By analyzing the phospho-Y162 level in metastatic tumors, we found that SMAD4 is highly phosphorylated in lung tumors derived from tumors expressing ERBB4 but not GFP or ERBB4 (K751M) (Figure 7F). These results suggest that ERBB4 fuels metastasis in a manner dependent on its kinase activity.

(D) *In vitro* kinase reaction was carried out by incubating recombinant GST-SMAD4 protein purified from *E. coli* and *in-vitro*-translated ERBB4 or K751M. SMAD4 phosphorylation was examined with the PY100 antibody.

(E) Schematic diagram of SMAD4 variants with different SMAD4 domains is shown. The binding activities of these variants to ERBB4, determined by *in vivo* coIP and kinase assay, are summarized. +, positive interaction or phosphorylation; -, negative binding or phosphorylation; n.d., not determined.

(F) Expression plasmids encoding FLAG-tagged ERBB4 or ERBB4 (K751M) and SFB-tagged SMAD4 were transfected into HEK293T cells. IP and western blotting were carried out. SMAD4 phosphorylation was examined with the PY162 antibody.

(G) Expression plasmids encoding HA-tagged ERBB4 and SFB-tagged wild-type SMAD4 or its Y162E, Y162F, Y114F, and Y117F mutants were co-transfected into HEK293T cells. IP and western blotting were carried out. SMAD4 phosphorylation was examined with the PY162 antibody.

(H) A549 cells stably expressing GFP or ERBB4 were lysed and then subjected to IP by anti-SMAD4 antibody or anti-IgG. Protein levels were examined by western blotting with indicated antibodies.

(I) H1299 cells with or without ERBB4 knockdown were subjected to IP and western blotting with indicated antibodies.

See also Figure S5.

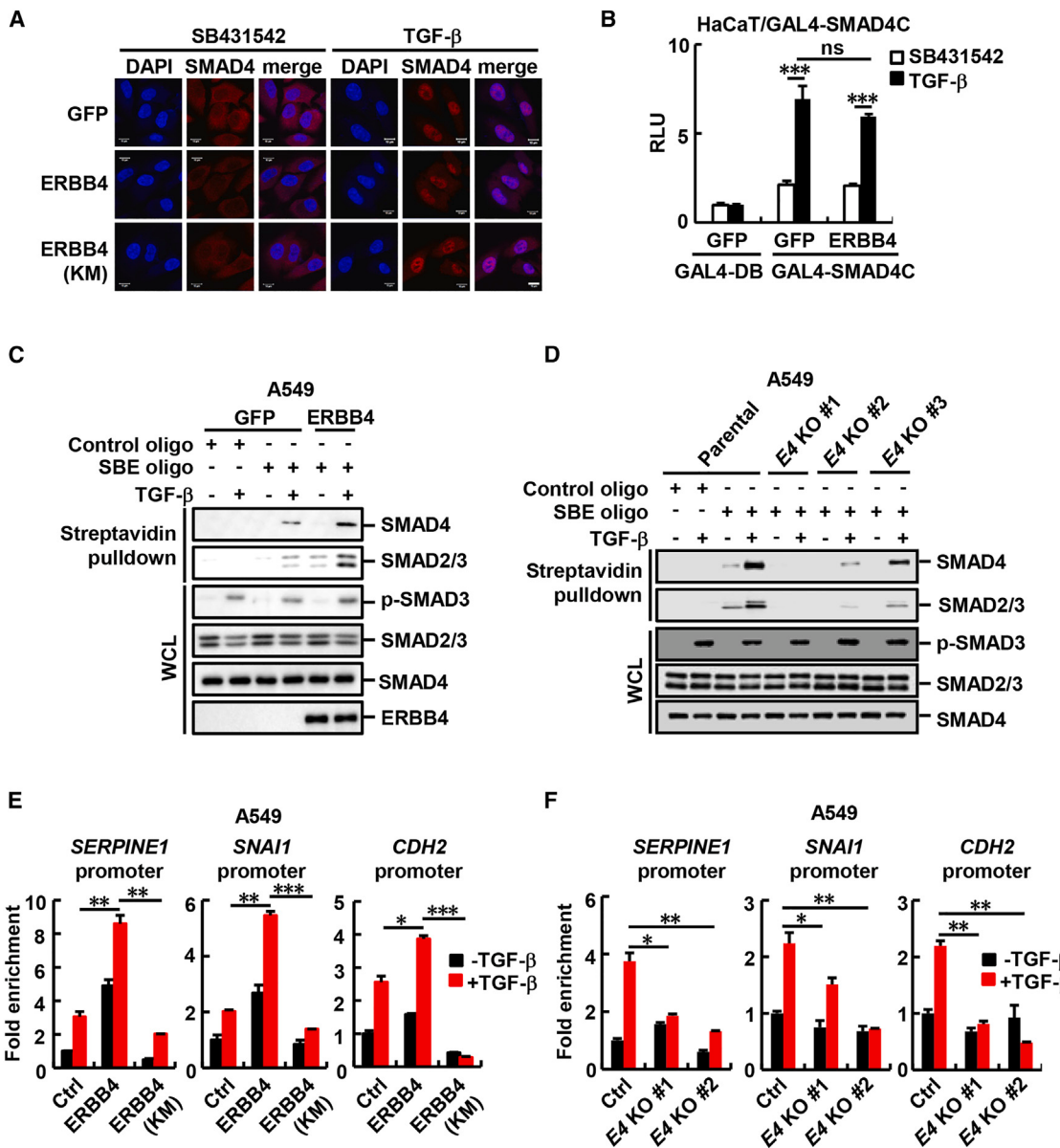


Figure 5. ERBB4 enhances the DNA-binding activity of SMAD4

(A) A549 cells stably expressing ERBB4 or ERBB4 (K751M) were treated with SB431542 (5 μ M) or TGF- β (2 ng/mL) for 2 h and then subjected to immunofluorescence with the indicated antibodies. Red, immunostained SMAD4; blue, 4',6-diamidino-2-phenylindole (DAPI) nuclear staining. Scale bars, 10 μ m.

(B) HaCaT cells were co-transfected with reporter plasmids pFR-luc and Renilla-luc, expression plasmids for ERBB4, and GAL4-SMAD4C (or GAL4 empty vector, GAL4-DB). Relative luciferase activities were measured after SB431542 (5 μ M) or TGF- β (2 ng/mL) treatment for 12 h.

(C) A549 cells stably expressing GFP or ERBB4 were treated with SB431542 (5 μ M) or TGF- β (2 ng/mL) for 2 h, and cell lysates were incubated with biotin-labeled SBE oligos followed by oligo precipitation with streptavidin beads. Co-precipitated proteins were determined by western blotting. The unlabeled SBE probe is a negative control.

(D) A549 parental and ERBB4-KO cells were treated with SB431542 (5 μ M) or TGF- β (2 ng/mL) for 2 h. The DNA-binding ability of SMAD4 was determined by a DNA pull-down assay as described in (C).

(E and F) A549 cells stably expressing ERBB4 or ERBB4 (K751M) (E) or with ERBB4 knockout (F) were treated with SB431542 (5 μ M) or TGF- β (2 ng/mL) for 8 h. ChIP and RT-qPCR analyses were carried out.

For all plots, data are shown as mean \pm SEM; $n = 3$. Statistical analysis was performed using a two-tailed Student's t test. * $p < 0.05$, ** $p < 0.01$, and *** $p < 0.001$. ns, non-significant.

See also Figure S6.

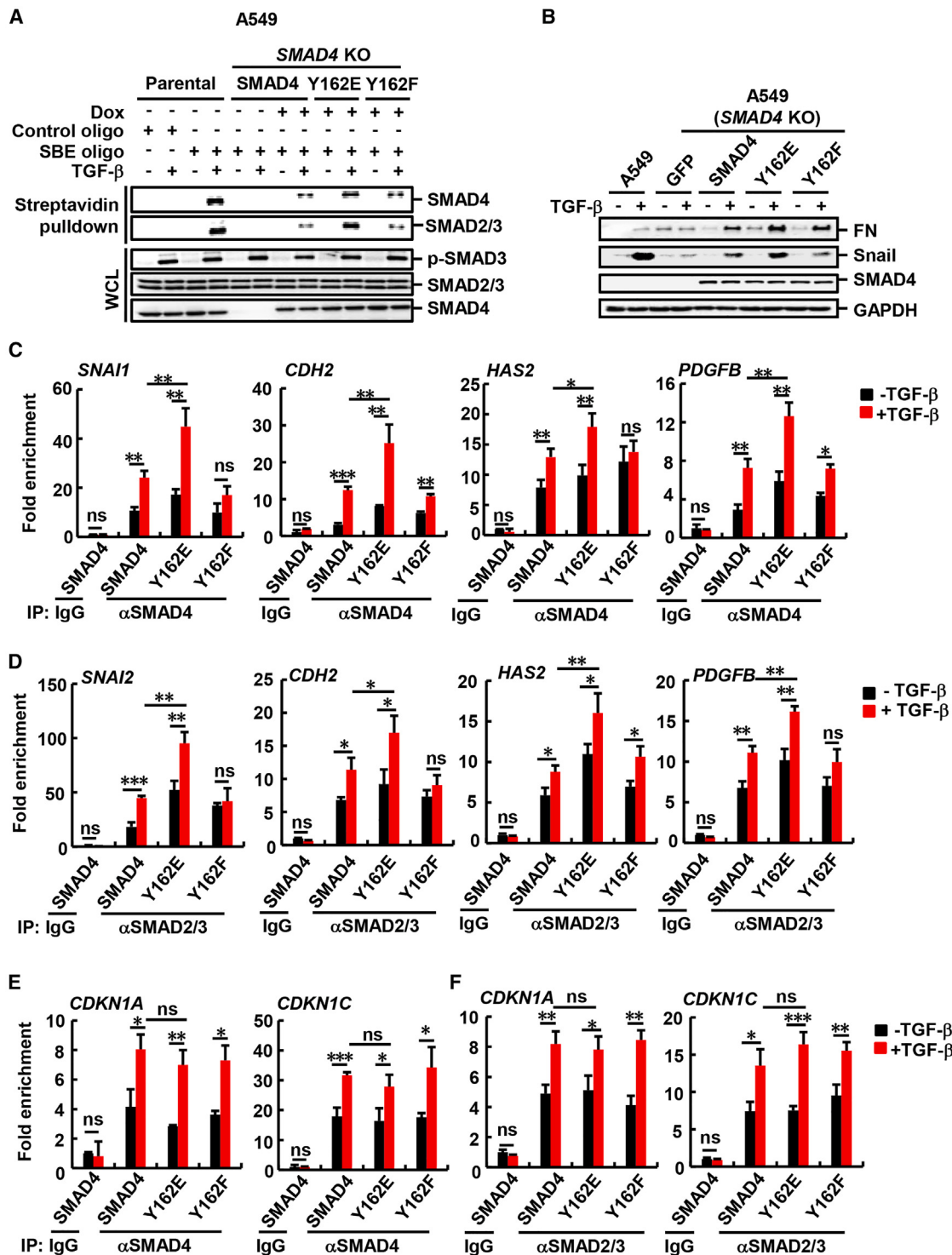


Figure 6. SMAD4 Y162 phosphorylation increases its binding to chromatin

(A) A549 parental and SMAD4-KO cells with inducible expression of SMAD4 (wild type [WT]/Y162E/Y162F) were pretreated with 0.1 ng/mL doxycycline (Dox) for 24 h and then supplemented with SB431542 (5 μ M) or TGF- β (2 ng/mL) for 2 h. Cell lysates were harvested, and a DNA pull-down assay was carried out.

(B) A549 parental and SMAD4-KO cells stably expressing GFP or SMAD4 (WT/Y162E/Y162F) were treated with SB431542 (5 μ M) or TGF- β (2 ng/mL) for 48 h. Cells were harvested and blotted with the indicated antibodies.

(legend continued on next page)

To investigate the impact of ERBB4-induced SMAD4 phosphorylation on tumor metastasis directly, we introduced wild-type SMAD4 or Y162 mutants into SMAD4-knockdown A549 cells. Subsequently, the cells were injected into the tail veins of NOD/SCID mice to stimulate lung metastasis. As expected, injecting control A549 cells (GFP, shCtrl) resulted in lung tumor metastasis (Figures 7G, 7H, and S7D). However, SMAD4 knockdown (shSMAD4) drastically reduced the lung metastasis, and this effect was reversed by reintroducing wild-type SMAD4 (Figures 7G, 7H, and S7D). Intriguingly, the Y162E mutant promoted metastasis more strongly than the wild-type SMAD4, whereas the Y162F mutant exhibited comparable metastatic potential to wild-type SMAD4 (Figures 7G, 7H, and S7D). These findings collectively demonstrate that ERBB4-mediated SMAD4 Y162 phosphorylation enhances lung cancer metastasis.

DISCUSSION

Multiple signaling pathways are converged to control tumor progression and metastasis. TGF- β cooperates with other signaling pathways, such as oncogenic Ras/RTK,¹⁵ to regulate the process of EMT. Studies have also indicated that ERBB family members, such as EGFR, HER2, and ERBB3, synergize with TGF- β signaling to modulate EMT via the MAPK pathway.^{20–23,32} However, the role of ERBB4 in tumorigenesis and its crosstalk with TGF- β signaling are not clear. In this study, we report that ERBB4 synergistically cooperates with SMAD4 to promote EMT and metastasis in response to TGF- β without affecting the cytostatic response of TGF- β . Our findings reveal a fresh mechanism underlying switching on TGF- β tumor-promoting signaling and contribute to the advancement of our current knowledge regarding the cooperation between RTKs and TGF- β in EMT and tumor metastasis (Figure 7I).

SMAD4 is a platform for oncogenic tyrosine phosphorylation

Despite TGF- β 's potent role in suppressing tumor growth and progression, it also paradoxically promotes processes like EMT, immune suppression, and microenvironment modifications that support tumor growth, survival, and metastasis. In cancer, numerous tyrosine kinases become activated and can influence the TGF- β signaling pathway. While tyrosine phosphorylation of the TGF- β signaling pathway is not typically observed under normal physiological conditions, aberrant activation of tyrosine kinases in cancer cells may impact TGF- β signaling. Our current study showing that ERBB4 causes SMAD4 tyrosine phosphorylation is consistent with the previous findings that SMAD4 is a target of tyrosine phosphorylation in ALK-positive solid tumors³³ and BCR-ABL1-positive chronic myeloid leukemia.³⁴ Thus, these findings suggest that SMAD4 phosphorylation could be a common regulatory mechanism for modulating

TGF- β signaling in cancers with active tyrosine kinases. While ALK or BCR-ABL1 blocks the tumor-suppressing function of SMAD4, ERBB4 specifically enhances the tumor-promoting role of SMAD4. Nonetheless, the tumor-suppressing or metastasis-promoting role of SMAD4 can be exploited by oncogenic kinases to promote tumorigenesis and malignancy. Moreover, considering the association between aberrant tyrosine kinase activities and tumorigenesis, it is plausible that tyrosine phosphorylation of SMAD4 by other hyperactive tyrosine kinases may occur in cancers lacking ERBB4, ALK, or BCR-ABL1 expression. This indicates that SMAD4 tyrosine phosphorylation could also potentially serve as a biomarker for diagnosing and prognosticating cancers.

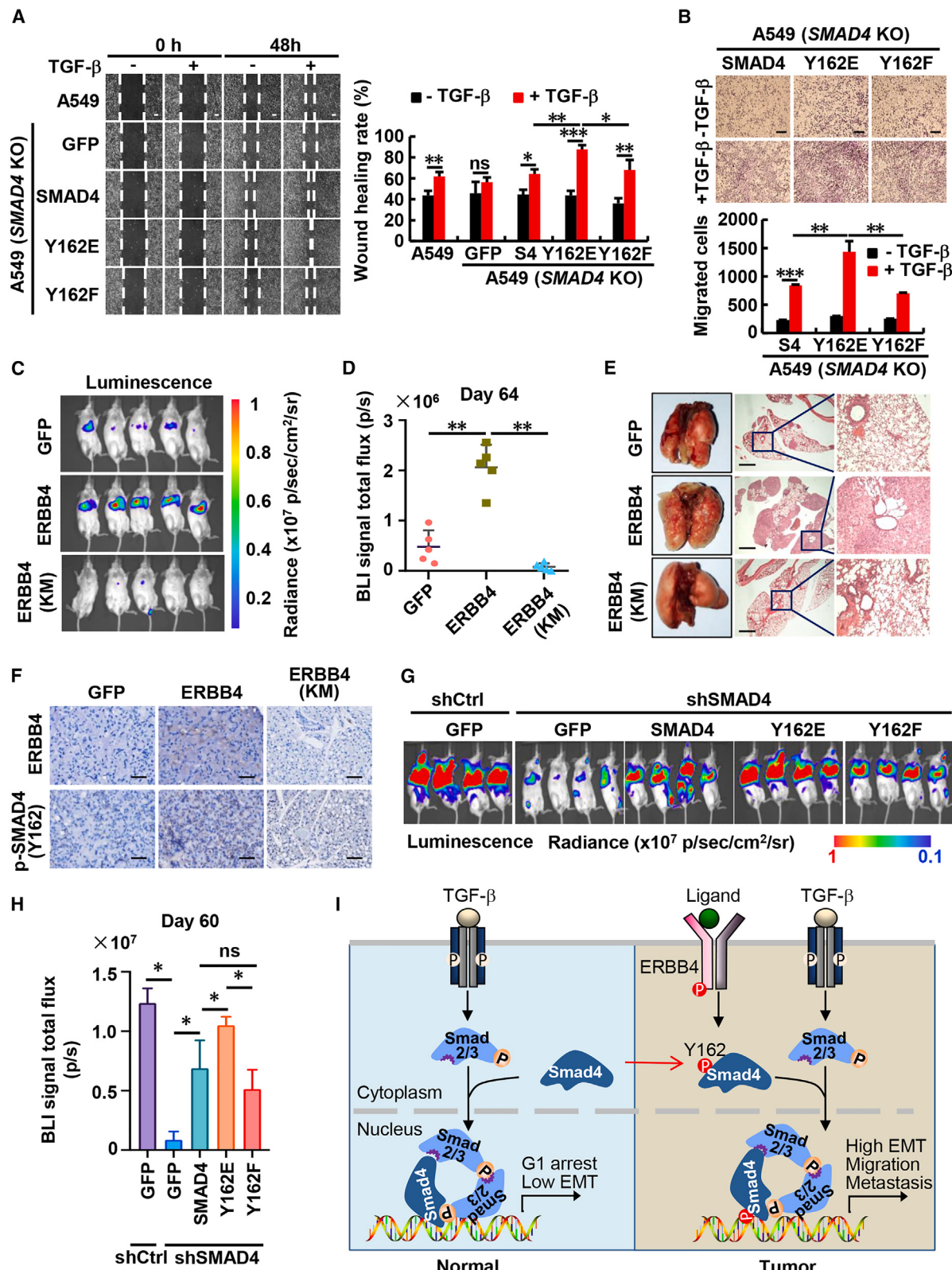
SMAD4 is phosphorylated by ERBB4 to mediate TGF- β 's metastasis-promoting ability without impacting its growth-inhibiting functions

Our mechanistic studies demonstrate that ERBB4 can directly interact with and phosphorylate Y162 in the linker region of SMAD4. Notably, due to the proximity of the Y162 site to the MH1 DNA-binding domain of SMAD4, ERBB4-mediated phosphorylation impacts the chromatin binding of SMAD4. Specifically, we found that ERBB4 augments the interaction between SMAD4 and chromatin. There are two noteworthy findings. First, the effect of ERBB4 is contrary to the effects of ALK- or BCR-ABL1-induced SMAD4 phosphorylation, which impairs SMAD4 DNA association or the recruitment of transcription coactivator p300/CBP, respectively.^{33,34} Second, the enhanced chromatin-binding activity of ERBB4-phosphorylated SMAD4 facilitates the expression of EMT-related genes induced by TGF- β but not its growth-inhibitory genes. These observations are rather interesting. Consequently, while ALK and BCR-ABL1 attenuate TGF- β 's tumor-suppressing function, contributing to ALK- or ABL1-driven tumorigenesis, ERBB4 specifically enhances the EMT- and metastasis-promoting role of SMAD4. However, it is unclear how the phosphorylation of SMAD4 on different residues, specifically Y162 by ERBB4 and Y95 by ALK, leads to distinct effects on chromatin binding and consequently impacts different gene sets. Given that SMAD proteins interact with context-dependent transcription factors, it is possible that phosphorylation at Y162 promotes the interaction of SMAD with transcription factors that favor EMT. This hypothesis needs to be explored further in future investigations. We have tested and found that SMAD4 Y162 phosphorylation does not affect the interactions of SMAD4 with RREB1 and INO80, two recently reported SMAD-interacting cofactors in enabling fibrogenic gene regulation,^{35,36} thereby ruling out the possible involvement of the two cofactors in ERBB4's differential regulation of TGF- β responses (data not shown). Nonetheless, the potential gain of DNA binding on the promoters of pro-metastasis genes due to phosphorylation at Y162 of SMAD4 aligns with the inherent role of ERBB4 in tumorigenesis.

(C–F) A549 SMAD4-KO cells stably expressing SMAD4 (WT/Y162E/Y162F) were treated with SB431542 (5 μ M) or TGF- β (2 ng/mL) for 8 h. ChIP and RT-qPCR analyses were carried out.

For all plots, data are shown as mean \pm SEM; $n = 3$. Statistical analysis was performed using a two-tailed Student's t test. * $p < 0.05$, ** $p < 0.01$, and *** $p < 0.001$. ns, non-significant.

See also Figure S6.



(legend on next page)

SMAD4 is a substrate of ERBB4 kinase to transduce ERBB4 signaling

Within the ERBB family of RTKs, EGFR and HER2 are recognized for their oncogenic roles and have been targeted in treating various solid tumors. On the other hand, ERBB4's role in human malignancies remains ambiguous. It exhibits conflicting behavior by functioning as an oncoprotein in some tumor types (e.g., brain, colon, stomach, head and neck, lung, bone, ovary, and thyroid) and as a tumor suppressor in others (e.g., bladder, liver, and prostate).³⁰ This paradoxical activity of ERBB4 may be attributed to its homotypic or heterotypic heterodimerization. Studies indicate that homotypic ERBB4 signaling leads to apoptosis, growth inhibition, and tumor suppression; however, heterotypic signaling through ERBB4-EGFR and ERBB4-ERBB2 heterodimers is associated with oncogenic behaviors like cell proliferation, migration, invasion, and resistance to chemotherapy.^{28,37} Considering the frequent overexpression of EGFR in NSCLC, it is plausible that ERBB4 contributes to the metastasis of lung cancer by forming ERBB4-EGFR heterodimers. Noteworthily, it has been observed that the kinase activity of ERBB4 may not be necessary for the growth-promoting effects of ERBB4 heterodimers.³⁸ Yet, our current study demonstrates that ERBB4 kinase activity is crucial for the pro-metastatic function of ERBB4 through, at least partly, phosphorylating SMAD4, a vital mediator of EMT. ERBB4 phosphorylates SMAD4 at Y162, which can be nullified by ERBB4 kinase inhibitors. Hence, discovering ERBB4 as a SMAD4 tyrosine kinase expands the range of ERBB4 substrates and reveals an interesting mode of regulating its oncogenic signaling. Although the study focused on lung cancer cells, these findings might be applicable to other cancers where ERBB4 confers metastatic potential, such as Ewing sarcoma.³⁹ Moreover, as targeting ERBB4 homodimeric signaling using small-molecule inhibitors could be deleterious, identifying SMAD4 as a previously unrecognized target of ERBB4 provides an alternative approach for targeting oncogenic ERBB4 heterodimers.

Limitations of the study

The study acknowledges several limitations that warrant further investigation. Firstly, while ERBB4-phosphorylated SMAD4 en-

hances the expression of TGF-β-induced EMT-related genes but not growth-inhibitory genes, the mechanism underlying this transcriptional selectivity remains unclear. Specifically, the role of SMAD4 Y162 phosphorylation in influencing the interaction between the SMAD complex and transcription factors that promote EMT should be explored. Secondly, it is yet to be determined if the phosphorylation of SMAD4 at Y162 significantly correlates with ERBB4 activity in human NSCLC patient samples. Should this correlation be absent, investigating alternative kinases that might phosphorylate this site could yield important insights into potential therapeutic targets. Lastly, the study's conclusions regarding the pro-metastatic activity of the ERBB4-SMAD4 regulatory axis are based on human cancer cell lines in a non-native mouse model. Therefore, further validation using more relevant models, such as spontaneous lung cancer models and endotracheal transplanted models, may be desired to substantiate these findings.

RESOURCE AVAILABILITY

Lead contact

Requests for further information and resources should be directed to and will be fulfilled by the lead contact, Xin-Hua Feng (fenglab@zju.edu.cn).

Materials availability

Plasmids, primers, cell lines, and data generated and described in this paper will be available upon reasonable request. Requests should be made to the lead contact.

Data and code availability

- Primer information is listed in [Table S1](#). Plasmid sequencing results, genotyping results, original blots, original images, and other original datasets are available upon request to the lead contact.
- This paper does not report the original code.
- Any additional information required to reanalyze the data reported in this work paper is available from the lead contact upon request.

ACKNOWLEDGMENTS

We thank Bert Vogelstein for SBE-luc, Norbert Fusenig for the HaCaT cell line, Weiwei Yang for the A549-luc cell line, and Hai Song and Jian Hu for other lung cell lines. We are grateful to the Core Facility of Life Sciences Institute and its staff for assisting with a variety of molecular and cellular analyses. We thank

Figure 7. Tyrosine phosphorylation enhances the pro-metastatic activity of SMAD4

(A and B) Cells were treated with or without 2 ng/mL TGF-β for 48 h, and the migration of cells was determined by wound-healing assay (A) and transwell assay (B). The migration rate was similarly quantitated and statistically analyzed as described in [Figures 1G](#) and [1H](#), respectively, shown in (A) (right) and (B) (bottom). Scale bars, 100 μm.

(C-E) Luciferase-expressing A549 cells stably expressing of GFP, ERBB4, or ERBB4 (K751M) were injected into NOD/SCID mice by tail vein injection ($n = 5$ per group), and 64 days after inoculation, bioluminescence imaging (BLI) was performed, and representative images of lung metastasis are shown (C). (D) BLI signals of mice in each experimental group at day 64. (E) Bright-field images of the lungs (left) and representative images of H&E staining of lung sections (right) 64 days after cell injection. Scale bars, 100 μm.

(F) Immunohistochemistry (IHC) staining of ERBB4 and p-SMAD4 (Y162) was performed in lung sections derived from A549 tumors expressing GFP, ERBB4, or ERBB4 (K751M). Scale bars, 25 μm.

(G and H) Luciferase-expressing, SMAD4-depleted A549 cells rescued with GFP, SMAD4 (WT), SMAD4 (Y162E), or SMAD4 (Y162F) were implanted into randomized NOD/SCID mice by tail vein injection ($n = 4$ per group), and 60 days after inoculation, BLI was performed, and representative images of lung metastasis are shown (G). (H) BLI signals of mice in each experimental group at day 60.

(I) A working model for the effect of tyrosine phosphorylation of SMAD4 on TGF-β signaling in ERBB4-positive tumors. Upon the aberrant activation of ERBB4 in tumors, SMAD4 is phosphorylated at Y162. Phosphorylated SMAD4 exhibits a stronger ability to bind DNA and elicit TGF-β-induced EMT, thereby promoting cancer metastasis.

For all plots, data are shown as mean ± SEM; $n = 3$. Statistical analysis was performed using a two-tailed Student's t test. * $p < 0.05$, ** $p < 0.01$, and *** $p < 0.001$. ns, non-significant.

See also [Figure S7](#).

members of the Feng Laboratory for helpful discussions and technical assistance. This research was partly supported by grants from the National Natural Science Foundation of China (U21A20356, 32321002, 31730057, and 81802627), the National Key Research and Development Program of China (2022YFC3401500), the Natural Science Foundation of Zhejiang Province (LD21C070001), the Hangzhou West Lake Pearl Project Leading Innovative Youth Team Project (TD2023017), and the Fundamental Research Funds for the Central Universities.

AUTHOR CONTRIBUTIONS

P.L. performed most of the experiments, analyzed data, and drafted the manuscript. J.C. was responsible for the xenograft tumor model. H.H., B.Z., J.L., S.Z., C.Y., J.C., J.W., Y.D., and Q.L. helped with some biochemical/cellular/animal experiments. P.X. and X. Liu provided key reagents. B.Y. performed the mass spectrometry experiment and data analyses. X. Lin initially conducted the antibody array screen and identified the SMAD4-ERBB4 interaction, analyzed data, and edited the manuscript. Y.Y. conducted and supervised experiments, analyzed data, and wrote the manuscript. X.-H.F. conceived and coordinated the study, supervised the experimental design, analyzed data, and wrote the manuscript.

DECLARATION OF INTERESTS

The authors declare no conflicts of interest.

STAR METHODS

Detailed methods are provided in the online version of this paper and include the following:

- KEY RESOURCES TABLE
- EXPERIMENTAL MODEL AND STUDY PARTICIPANT DETAILS
 - Animals
 - Cell culture and transfection
- METHOD DETAILS
 - Plasmid construction
 - Quantitative reverse-transcription PCR (RT-qPCR)
 - Generation of SMAD4 or ERBB4 knockout cells
 - Immunoprecipitation and western blotting analysis
 - GST pulldown assay
 - *In vitro* phosphorylation assay
 - Luciferase reporter assay
 - Immunofluorescence
 - Nuclear and cytosolic fractionation
 - GAL4 transactivation assay
 - Mass spectrometry analysis
 - DNA pulldown assay
 - ChIP assay
 - Wound healing assay
 - Transwell migration assay
 - Cell proliferation and cell cycle assays
 - Mouse tumor model
 - IHC analysis
- QUANTIFICATION AND STATISTICAL ANALYSIS

SUPPLEMENTAL INFORMATION

Supplemental information can be found online at <https://doi.org/10.1016/j.celrep.2024.115210>.

Received: June 19, 2024

Revised: November 19, 2024

Accepted: December 24, 2024

Published: January 23, 2025

REFERENCES

1. Lee, J.H., and Massagué, J. (2022). TGF-beta in developmental and fibrogenic EMTs. *Semin. Cancer Biol.* 86, 136–145. <https://doi.org/10.1016/j.semancer.2022.09.004>.
2. Katsuno, Y., and Deryck, R. (2021). Epithelial plasticity, epithelial-mesenchymal transition, and the TGF-beta family. *Dev. Cell* 56, 726–746. <https://doi.org/10.1016/j.devcel.2021.02.028>.
3. Kahata, K., Dadras, M.S., and Moustakas, A. (2018). TGF- β Family Signaling in Epithelial Differentiation and Epithelial-Mesenchymal Transition. *Cold Spring Harbor Perspect. Biol.* 10, a022194. <https://doi.org/10.1101/cshperspect.a022194>.
4. Liu, S., Ren, J., and Ten Dijke, P. (2021). Targeting TGF β signal transduction for cancer therapy. *Signal Transduct. Targeted Ther.* 6, 8. <https://doi.org/10.1038/s41392-020-00436-9>.
5. Yu, Y., and Feng, X.H. (2019). TGF-beta signaling in cell fate control and cancer. *Curr. Opin. Cell Biol.* 61, 56–63. <https://doi.org/10.1016/j.ceb.2019.07.007>.
6. Morikawa, M., Deryck, R., and Miyazono, K. (2016). TGF- β and the TGF- β Family: Context-Dependent Roles in Cell and Tissue Physiology. *Cold Spring Harbor Perspect. Biol.* 8, a021873. <https://doi.org/10.1101/cshperspect.a021873>.
7. Batlle, E., and Massagué, J. (2019). Transforming Growth Factor- β Signaling in Immunity and Cancer. *Immunity* 50, 924–940. <https://doi.org/10.1016/j.immuni.2019.03.024>.
8. Deryck, R., Turley, S.J., and Akhurst, R.J. (2021). TGF β biology in cancer progression and immunotherapy. *Nat. Rev. Clin. Oncol.* 18, 9–34. <https://doi.org/10.1038/s41571-020-0403-1>.
9. Chen, W., and Ten Dijke, P. (2016). Immunoregulation by members of the TGF β superfamily. *Nat. Rev. Immunol.* 16, 723–740. <https://doi.org/10.1038/nri.2016.112>.
10. Feng, X.H., and Deryck, R. (2005). Specificity and versatility in tgf-beta signaling through Smads. *Annu. Rev. Cell Dev. Biol.* 21, 659–693. <https://doi.org/10.1146/annurev.cellbio.21.022404.142018>.
11. Lu, W., and Kang, Y. (2019). Epithelial-Mesenchymal Plasticity in Cancer Progression and Metastasis. *Dev. Cell* 49, 361–374. <https://doi.org/10.1016/j.devcel.2019.04.010>.
12. David, C.J., and Massague, J. (2018). Contextual determinants of TGFbeta action in development, immunity and cancer. *Nat. Rev. Mol. Cell Biol.* 19, 419–435. <https://doi.org/10.1038/s41580-018-0007-0>.
13. Moustakas, A., and Heldin, C.H. (2016). Mechanisms of TGF β -Induced Epithelial-Mesenchymal Transition. *J. Clin. Med.* 5, 63. <https://doi.org/10.3390/jcm5070063>.
14. Miyazono, K., Katsuno, Y., Koinuma, D., Ehata, S., and Morikawa, M. (2018). Intracellular and extracellular TGF- β signaling in cancer: some recent topics. *Front. Med.* 12, 387–411. <https://doi.org/10.1007/s11684-018-0646-8>.
15. Grünert, S., Jechlinger, M., and Beug, H. (2003). Diverse cellular and molecular mechanisms contribute to epithelial plasticity and metastasis. *Nat. Rev. Mol. Cell Biol.* 4, 657–665. <https://doi.org/10.1038/nrm1175>.
16. Shi, Q., and Chen, Y.G. (2017). Interplay between TGF-beta signaling and receptor tyrosine kinases in tumor development. *Sci. China Life Sci.* 60, 1133–1141. <https://doi.org/10.1007/s11427-017-9173-5>.
17. Hao, Y., Baker, D., and Ten Dijke, P. (2019). TGF- β -Mediated Epithelial-Mesenchymal Transition and Cancer Metastasis. *Int. J. Mol. Sci.* 20, 2767. <https://doi.org/10.3390/ijms20112767>.
18. Hua, W., Ten Dijke, P., Kostidis, S., Giera, M., and Hornsveld, M. (2020). TGF β -induced metabolic reprogramming during epithelial-to-mesenchymal transition in cancer. *Cell. Mol. Life Sci.* 77, 2103–2123. <https://doi.org/10.1007/s0018-019-03398-6>.
19. Ganesh, K., and Massagué, J. (2021). Targeting metastatic cancer. *Nat. Med.* 27, 34–44. <https://doi.org/10.1038/s41591-020-01195-4>.

20. Zhao, Y., Ma, J., Fan, Y., Wang, Z., Tian, R., Ji, W., Zhang, F., and Niu, R. (2018). TGF-beta transactivates EGFR and facilitates breast cancer migration and invasion through canonical Smad3 and ERK/Sp1 signaling pathways. *Mol. Oncol.* 12, 305–321. <https://doi.org/10.1002/1878-0261.12162>.
21. Wendt, M.K., Smith, J.A., and Schiemann, W.P. (2010). Transforming growth factor-beta-induced epithelial-mesenchymal transition facilitates epidermal growth factor-dependent breast cancer progression. *Oncogene* 29, 6485–6498. <https://doi.org/10.1038/onc.2010.377>.
22. Huang, F., Shi, Q., Li, Y., Xu, L., Xu, C., Chen, F., Wang, H., Liao, H., Chang, Z., Liu, F., et al. (2018). HER2/EGFR-AKT signaling switches TGF β from inhibiting cell proliferation to promoting cell migration in breast cancer. *Cancer Res.* 78, 6073–6085. <https://doi.org/10.1158/0008-5472.CAN-18-0136>.
23. Kim, J., Jeong, H., Lee, Y., Kim, C., Kim, H., and Kim, A. (2013). HRG- β 1-driven ErbB3 signaling induces epithelial-mesenchymal transition in breast cancer cells. *BMC Cancer* 13, 383. <https://doi.org/10.1186/1471-2407-13-383>.
24. Lee, H.W., Khan, S.Q., Khalidina, S., Altintas, M.M., Grahammer, F., Zhao, J.L., Koh, K.H., Tardi, N.J., Faridi, M.H., Geraghty, T., et al. (2017). Absence of miR-146a in Podocytes Increases Risk of Diabetic Glomerulopathy via Up-regulation of ErbB4 and Notch-1. *J. Biol. Chem.* 292, 732–747. <https://doi.org/10.1074/jbc.M116.753822>.
25. Kim, T.Y., Han, H.S., Lee, K.W., Zang, D.Y., Rha, S.Y., Park, Y.I., Kim, J.S., Lee, K.H., Park, S.H., Song, E.K., et al. (2019). A phase I/II study of poziotinib combined with paclitaxel and trastuzumab in patients with HER2-positive advanced gastric cancer. *Gastric Cancer* 22, 1206–1214. <https://doi.org/10.1007/s10120-019-00958-4>.
26. Roskoski, R., Jr. (2021). Orally effective FDA-approved protein kinase targeted covalent inhibitors (TCIs). *Pharmacol. Res.* 165, 105422. <https://doi.org/10.1016/j.phrs.2021.105422>.
27. Zhang, J., Cao, J., Li, J., Zhang, Y., Chen, Z., Peng, W., Sun, S., Zhao, N., Wang, J., Zhong, D., et al. (2014). A phase I study of AST1306, a novel irreversible EGFR and HER2 kinase inhibitor, in patients with advanced solid tumors. *J. Hematol. Oncol.* 7, 1–11. <https://doi.org/10.1186/1756-8722-7-22>.
28. Segers, V.F.M., Dugaucquier, L., Feyen, E., Shakeri, H., and De Keulenaer, G.W. (2020). The role of ErbB4 in cancer. *Cell. Oncol.* 43, 335–352. <https://doi.org/10.1007/s13402-020-00499-4>.
29. Lee, J.H., and Massagué, J. (2022). TGF- β in developmental and fibrogenic EMTs. *Semin. Cancer Biol.* 86, 136–145. <https://doi.org/10.1016/j.semcan.2022.09.004>.
30. Lucas, L.M., Dwivedi, V., Senfeld, J.I., Cullum, R.L., Mill, C.P., Piazza, J.T., Bryant, I.N., Cook, L.J., Miller, S.T., Lott, J.H., 4th, et al. (2022). The Yin and Yang of ERBB4: Tumor Suppressor and Oncoprotein. *Pharmacol. Rev.* 74, 18–47. <https://doi.org/10.1124/pharmrev.121.000381>.
31. Liu, J., Zhao, M., Yuan, B., Gu, S., Zheng, M., Zou, J., Jin, J., Liu, T., and Feng, X.H. (2018). WDR74 functions as a novel coactivator in TGF- β signaling. *J. Genet. Genomics.* 45, 639–650. <https://doi.org/10.1016/j.jgg.2018.08.005>.
32. Seton-Rogers, S.E., Lu, Y., Hines, L.M., Koundinya, M., LaBaer, J., Muthuswamy, S.K., and Brugge, J.S. (2004). Cooperation of the ErbB2 receptor and transforming growth factor beta in induction of migration and invasion in mammary epithelial cells. *Proc. Natl. Acad. Sci. USA* 101, 1257–1262. <https://doi.org/10.1073/pnas.0308090100>.
33. Zhang, Q., Xiao, M., Gu, S., Xu, Y., Liu, T., Li, H., Yu, Y., Qin, L., Zhu, Y., Chen, F., et al. (2019). ALK phosphorylates SMAD4 on tyrosine to disable TGF-beta tumour suppressor functions. *Nat. Cell Biol.* 21, 179–189. <https://doi.org/10.1038/s41556-018-0264-3>.
34. Wang, L., Gu, S., Chen, F., Yu, Y., Cao, J., Li, X., Gao, C., Chen, Y., Yuan, S., Liu, X., et al. (2023). Imatinib blocks tyrosine phosphorylation of Smad4 and restores TGF- β growth-suppressive signaling in BCR-ABL1-positive leukemia. *Signal Transduct. Targeted Ther.* 8, 120. <https://doi.org/10.1038/s41392-023-01327-5>.
35. Su, J., Morgani, S.M., David, C.J., Wang, Q., Er, E.E., Huang, Y.H., Basnet, H., Zou, Y., Shu, W., Soni, R.K., et al. (2020). TGF-beta orchestrates fibrogenic and developmental EMTs via the RAS effector RREB1. *Nature* 577, 566–571. <https://doi.org/10.1038/s41586-019-1897-5>.
36. Lee, J.H., Sanchez-Rivera, F.J., He, L., Basnet, H., Chen, F.X., Spina, E., Li, L., Torner, C., Chan, J.E., Yarlagadda, D.V.K., et al. (2024). TGF-beta and RAS jointly unmask primed enhancers to drive metastasis. *Cell* 187, 6182–6199. <https://doi.org/10.1016/j.cell.2024.08.014>.
37. Mill, C.P., Gettinger, K.L., and Riese, D.J., 2nd. (2011). Ligand stimulation of ErbB4 and a constitutively-active ErbB4 mutant result in different biological responses in human pancreatic tumor cell lines. *Exp. Cell Res.* 317, 392–404. <https://doi.org/10.1016/j.yexcr.2010.11.007>.
38. Wilson, K.J., Mill, C.P., Gallo, R.M., Cameron, E.M., VanBrocklin, H., Settleman, J., and Riese, D.J. (2012). The Q43L mutant of neuregulin 2 β is a pan-ErbB receptor antagonist. *Biochem. J.* 443, 133–144. <https://doi.org/10.1042/BJ20110921>.
39. Mendoza-Naranjo, A., El-Nagar, A., Wai, D.H., Mistry, P., Lazic, N., Ayala, F.R.R., da Cunha, I.W., Rodriguez-Viciano, P., Cheng, H., Tavares Guerreiro Fregnani, J.H., et al. (2013). ERBB4 confers metastatic capacity in Ewing sarcoma. *EMBO Mol. Med.* 5, 1087–1102. <https://doi.org/10.1002/emmm.201202343>.
40. Zawel, L., Dai, J.L., Buckhaults, P., Zhou, S., Kinzler, K.W., Vogelstein, B., and Kern, S.E. (1998). Human Smad3 and Smad4 are sequence-specific transcription activators. *Mol. Cell* 1, 611–617. [https://doi.org/10.1016/s1097-2765\(00\)80061-1](https://doi.org/10.1016/s1097-2765(00)80061-1).
41. Dennler, S., Itoh, S., Vivien, D., ten Dijke, P., Huet, S., and Gauthier, J.M. (1998). Direct binding of Smad3 and Smad4 to critical TGF beta-inducible elements in the promoter of human plasminogen activator inhibitor-type 1 gene. *EMBO J.* 17, 3091–3100. <https://doi.org/10.1093/emboj/17.11.3091>.
42. Feng, X.H., Zhang, Y., Wu, R.Y., and Deryck, R. (1998). The tumor suppressor Smad4/DPC4 and transcriptional adaptor CBP/p300 are coactivators for smad3 in TGF-beta-induced transcriptional activation. *Genes Dev.* 12, 2153–2163. <https://doi.org/10.1101/gad.12.14.2153>.
43. Lin, X., Duan, X., Liang, Y.Y., Su, Y., Wrighton, K.H., Long, J., Hu, M., Davis, C.M., Wang, J., Brunicardi, F.C., et al. (2006). PPM1A functions as a Smad phosphatase to terminate TGFbeta signaling. *Cell* 125, 915–928. <https://doi.org/10.1016/j.cell.2006.03.044>.
44. Yu, Y., Gu, S., Li, W., Sun, C., Chen, F., Xiao, M., Wang, L., Xu, D., Li, Y., Ding, C., et al. (2017). Smad7 enables STAT3 activation and promotes pluripotency independent of TGF-beta signaling. *Proc. Natl. Acad. Sci. USA* 114, 10113–10118. <https://doi.org/10.1073/pnas.1705755114>.
45. Liu, T., Zhao, M., Liu, J., He, Z., Zhang, Y., You, H., Huang, J., Lin, X., and Feng, X.H. (2017). Tumor suppressor bromodomain-containing protein 7 cooperates with Smads to promote transforming growth factor-beta responses. *Oncogene* 36, 362–372. <https://doi.org/10.1038/onc.2016.204>.
46. Zhao, Y., Liu, J., Chen, F., and Feng, X.H. (2018). C-terminal domain small phosphatase-like 2 promotes epithelial-to-mesenchymal transition via Snail dephosphorylation and stabilization. *Open Biol.* 8, 170274. <https://doi.org/10.1098/rsob.170274>.

STAR★METHODS

KEY RESOURCES TABLE

REAGENT or RESOURCE	SOURCE	IDENTIFIER
Antibodies		
Phospho-ERBB4 (Tyr1284)	Cell Signaling Technology	Cat# 4757; RRID: AB_2099987
ERBB4	Abcam	Cat# ab32375; RRID: AB_731579
SMAD4 (D3M6U)	Cell Signaling Technology	Cat# 38454; RRID: AB_2728776
SMAD4 (D3R4N)	Cell Signaling Technology	Cat# 46535; RRID: AB_2736998
SMAD2/3	Cell Signaling Technology	Cat# 8685; RRID: AB_10889933
SMAD3	Cell Signaling Technology	Cat# 9523; RRID: AB_2193182
<i>p</i> -SMAD3 (Ser423/425)	Cell Signaling Technology	Cat# 9520; RRID: AB_2193207
<i>p</i> -Tyr-100	Cell Signaling Technology	Cat# 9411; RRID: AB_331228
Monoclonal ANTI-FLAG M2 antibody	Sigma-Aldrich	Cat#F3165; RRID: AB_259
HA-tag	Cell Signaling Technology	Cat# 3724; RRID: AB_1549585
HA-tag	Santa Cruz Biotechnology	Cat# 7392; RRID: AB_2894930
MYC-tag	Cell Signaling Technology	Cat# 2276; RRID: AB_3317
anti-rabbit IgG, HRP-linked Antibody	Cell Signaling Technology	Cat# 7074; RRID: AB_2099233
Snail	Cell Signaling Technology	Cat# 3879; RRID: AB_10828214
Slug	Cell Signaling Technology	Cat# 9585; RRID: AB_2239535
PAI-1	Santa Cruz Biotechnology	Cat# 5297; RRID: AB_628154
Fibronectin	Santa Cruz Biotechnology	Cat# 8422; RRID: AB_627598
N-Cadherin	Santa Cruz Biotechnology	Cat# 59987; RRID: AB_78174
p21 Waf1/Cip1 (12D1)	Cell Signaling Technology	Cat# 2947; RRID: AB_823586
c-Myc (D84C12)	Cell Signaling Technology	Cat# 5605; RRID: AB_1903938
Lamin A/C	Santa Cruz Biotechnology	Cat# 59987; RRID: AB_627874
GAPDH	Sigma-Aldrich	Cat# G8795; RRID: AB_1078991
Alexa Fluor 546 donkey anti-rabbit IgG	Thermo Fisher Scientific	Cat# A10040; RRID: AB_2534016
Alexa Fluor 488 donkey anti-rabbit IgG	Thermo Fisher Scientific	Cat# A32790; RRID: AB_2762833
SMAD4 PY162 antibody against (MVKDEpYVHDLEGQPC)	HuaBio (Hangzhou) Ltd	N/A
Biotin-SP (long spacer) AffiniPure Goat Anti-Mouse IgG (H + L)	Jackson ImmunoResearch	115-065-003; RRID: AB_2338557
Biotin-SP (long spacer) AffiniPure Goat Anti-Rabbit IgG (H + L)	Jackson ImmunoResearch	111-065-003; RRID: AB_2337959
Chemicals, peptides, and recombinant proteins		
recombinant human TGF- β 1	StemRD	Cat# TGB1-100
SB431542	Sigma-Aldrich	Cat# S4317
Afatinib	TargetMol	Cat# T2303
AST-1306	TargetMol	Cat# T6331
Pozotinib	TargetMol	Cat# T2630
Insulin	Sigma-Aldrich	Cat# I1882
EGF	Sigma-Aldrich	Cat# E9644
Cholera toxin	Sigma-Aldrich	Cat# C8052
Hydrocortison	Sigma-Aldrich	Cat# H0888

(Continued on next page)

Continued

REAGENT or RESOURCE	SOURCE	IDENTIFIER
DAPI	BioLegend	Cat# 422801
Puromycin	Merck	Cat# 540411
Lipofectamine 3000 transfection reagent	Invitrogen	Cat# L3000075
X-tremeGENE HP DNA Transfection Reagent	Roche Applied Science	Cat# 6366236001
Opti-MEM Reduced Serum Medium	GIBCO	Cat# 31985070
TRIzol	Invitrogen	Cat# 15596018
Fetal Bovine Serum	Hyclone	Cat# SH30396.03
Horse Serum	GIBCO	Cat# 16050122
RPMI 1640 medium	Sigma-Aldrich	Cat# R8758
MEM-EBSS medium	Sigma-Aldrich	Cat# M4655
DMEM/F12 medium	Sigma-Aldrich	Cat# D8437
DMEM medium	Sigma-Aldrich	Cat# D6429
LHC-8 medium	GIBCO	Cat# 12678017
Polybrene	Sigma-Aldrich	Cat# H9268
5 × Passive Lysis Buffer	Promega Corporation	Cat# E194A
Critical commercial assays		
6.5 mm Transwell® with 8.0 µm Pore Polycarbonate Membrane Insert	Corning	Cat# CLS3422
TNT® SP6 Quick Coupled Transcription/Translation System	Promega	Cat# L2080
Pierce™ Agarose ChIP Kit	Thermo Fisher Scientific	Cat# 26156
Cell-Light EdU Apollo567 <i>In Vitro</i> Kit	RiboBio	Cat# C10310-1
Cell Cycle and Apoptosis Analysis Kit	Beyotime	Cat# C1052
PrimeScript™ RT Master Mix	Takara Bio	Cat# RR036A
PowerUp SYBR Green Master Mix	Thermo Fisher Scientific	Cat# A25743
Protein A-Sepharose® CL-4B	GE HealthCare Lifesciences	Cat# 7078001
Streptavidin Sepharose High Performance	GE HealthCare Lifesciences	Cat# 17511301
Dual-Luciferase Reporter Assay System	Promega	Cat# E1910
Peroxidase Streptavidin	Jackson ImmunoResearch	Cat# 016-030-084; RRID: AB_2337238
Metal Enhanced DAB Substrate Kit	Solarbio LIFE SCIENCES	Cat# DA1016
Experimental models: Cell lines		
HEK293T	ATCC	CRL-3216
A549	Cell library of the Chinese Academy of Sciences	CSTR:19375.09.3101HUMSCSP503
A549-luc	Laboratory of Weiwei Yang	N/A
H1299	Laboratory of Hai Song	N/A
Clau-3	Cell library of the Chinese Academy of Sciences	CSTR:19375.09.3101HUMTCHu157
SPC-A-1	Laboratory of Jian Hu	N/A
HaCaT	Laboratory of Norbert Fusenig	N/A
MCF10A	ATCC	CRL-10317
BEP2D	Laboratory of Hai Song	N/A
A549 (GFP/ERBB4/K751M-stable)	This paper	N/A
A549 (ERBB4-KD/KO)	This paper	N/A
A549 (ERBB4-KD & Rescue rERBB4)	This paper	N/A
A549 (SMAD4-KD/KO)	This paper	N/A

(Continued on next page)

Continued

REAGENT or RESOURCE	SOURCE	IDENTIFIER
A549 (SMAD4-KO & Rescue SMAD4 mutants)	This paper	N/A
A549 (SMAD4-KO & Rescue ERBB4)	This paper	N/A
A549-luc (GFP/ERBB4/K751M-stable)	This paper	N/A
A549-luc (ERBB4-KD)	This paper	N/A
A549-luc (SMAD4-KD & Rescue SMAD4 mutants)	This paper	N/A
H1299 (ERBB4-KD)	This paper	N/A
Clau-3 (ERBB4-KD)	This paper	N/A
SPC-A-1 (ERBB4-KD)	This paper	N/A
HaCaT (GFP/ERBB4-stable)	This paper	N/A
HaCaT (ERBB4-KD)	This paper	N/A
MCF10A (GFP/ERBB4/K751M-stable)	This paper	N/A
BEP2D (GFP/ERBB4-stable)	This paper	N/A
BEP2D (ERBB4-KD)	This paper	N/A
Experimental models: Organisms/strains		
female NOD SCID mice	Shanghai SLAC Laboratory Animal Co. Ltd	N/A
Oligonucleotides		
Primers used in this study, see Table S1	This paper	N/A
Recombinant DNA		
pLKO.1	Addgene	Cat# 24150
lenti-CRISPRv2	Addgene	Cat# 52961
SBE-luc	Zawel et al. ⁴⁰	N/A
CAGA-luc	Dennler et al. ⁴¹	N/A
MYC-tagged SMAD4 truncations	This study	N/A
FLAG-tagged SMAD4 truncations	Wang et al. ³⁴	N/A
GAL4-DB/GAL4-SMAD4C/pFR-Luc	Liu et al. ³¹	N/A
GST-SMAD4	Feng et al. ⁴²	N/A
pRK5F-SMAD4-FLAG	This study	N/A
pRK5F-ERBB4-FLAG	This study	N/A
pRK5F-ERBB4 (K751M)-FLAG	This study	N/A
pRK5F-SMAD4 (Y114 E/F)-FLAG	This study	N/A
pRK5F-SMAD4 (Y117 E/F)-FLAG	This study	N/A
pRK5F-SMAD4 (Y162 E/F)-FLAG	This study	N/A
pRK5F-SMAD4 (Y353 E/F)-FLAG	This study	N/A
pRK5F-SMAD4 (Y412 E/F)-FLAG	This study	N/A
pRK5F-SMAD4 (Y513 E/F)-FLAG	This study	N/A
pRK-SFB-SMAD4 (WT/Y162 E/F)-FLAG	This study	N/A
pRK5F-ERBB4-ICD-FLAG	This study	N/A
pRK3H-ERBB4-HA	This study	N/A
pRK3H-ERBB4 (K751M)-HA	This study	N/A
pWPI-ERBB4-FLAG	This study	N/A
pWPI-ERBB4 (K751M)-FLAG	This study	N/A
pInducer-SMAD4 (WT/Y162 E/F)-FLAG	This study	N/A
pLKO.1-shERBB4-1	This study	N/A
pLKO.1-shERBB4-2	This study	N/A
pLKO.1-shSMAD4	This study	N/A
CRISPRv2-ERBB4 sgRNA #1	This study	N/A
CRISPRv2-ERBB4 sgRNA #2	This study	N/A

(Continued on next page)

Continued

REAGENT or RESOURCE	SOURCE	IDENTIFIER
CRISPRv2-ERBB4 sgRNA #3	This study	N/A
CRISPRv2-SMAD4 sgRNA	This study	N/A
Software and algorithms		
GraphPad Prism	GraphPad Software	https://www.graphpad.com/
ImageJ	National Institutes of Health	https://imagej.net/ij/
Image Lab	BioRad	N/A
NIS-Elements	Nikon	N/A
AxioVision	Zeiss	N/A
Zen	Zeiss	N/A

EXPERIMENTAL MODEL AND STUDY PARTICIPANT DETAILS

Animals

For tail vein metastasis assay, seven-week-old female NOD SCID mice (at the beginning of the assay) were used. Mice were purchased from Shanghai SLAC Laboratory Animal Co. Ltd at six-week-of-age, and were fed on site for one week before subjected to the assay. All mice were maintained in pathogen-free facilities at Zhejiang University. Animal protocols used in the study were supervised by Zhejiang University Committee for Experimental Animal Studies and Ethics (No. 16896) and all animal experiments conform to the relevant regulatory standards. Animal welfare regulations, environmental protection and biorisk-related regulations in the local research setting were sufficient.

Cell culture and transfection

HEK293T cells were cultured in DMEM medium (Sigma) supplemented with 10% fetal bovine serum (FBS) (HyClone). SPC-A-1, and A549 cells were cultured in RPMI-1640 medium (Sigma) with 10% FBS. H1299 cells were cultured in RPMI-1640 medium with 10% FBS and 1% Sodium Pyruvate (Gibco). Calu-3 and HaCaT cells were cultured in MEM-EBSS medium (Sigma) with 10% FBS and 1% Sodium Pyruvate. BEP2D cells were cultured in serum-free LHC-8 medium (Gibco). MCF10A cells were cultured in DMEM/F12 medium (Sigma) supplemented with 5% horse serum (Invitrogen), insulin (10 µg/mL), EGF (20 ng/mL), cholera toxin (100 ng/mL) (Sigma), and hydrocortisone (0.5 µg/mL) (Sigma). All cells were cultured in 37°C incubator with 5% CO₂. Among these cell lines, MCF10A cells were derived from female, SPC-A-1, A549, H1299, Calu-3, HaCaT cells were derived from male. We did not acquire sex information about other cell lines. HaCaT cells were transfected with X-tremeGENE (Roche Applied Science); A549 cells were transfected with Lipofectamine 3000 (Invitrogen), and HEK293T cells were transfected with PEI (Polyscience).

METHOD DETAILS

Plasmid construction

Full-length ERBB4 cDNA, kinase-dead ERBB4 (K751M, KD) and SMAD4 mutants (Y162 E/F, Y114 E/F, Y117 E/F, Y353 E/F, Y412 E/F and Y513 E/F) were produced by PCR or PCR-based mutagenesis and confirmed by sequencing. The intracellular domain of ERBB4 (4ICD) was generated by PCR. The above ERBB4 or SMAD4 cDNAs were subcloned into mammalian expression vectors pRK5F (FLAG tag), pRK3H (HA tag), or pRK-SFB (SFB tag, which contains a combined S protein tag, FLAG tag and Streptavidin binding peptide). Lentiviral tet-on expression plasmids for SMAD4, SMAD4 (Y162E) and SMAD4 (Y162F) were constructed by subcloning into plenti-Inducer. Lentiviral constitutive expression plasmids for FLAG-tagged SMAD4, SMAD4 (Y162E), SMAD4 (Y162F), ERBB4 and ERBB4 (KD) were constructed by subcloning into pWPI-Puro-IRES-GFP. FLAG-tagged SMAD4 truncations³⁴ and GST-SMAD4 fusion constructs⁴² were previously reported. shRNA or non-specific control was cloned into the pLKO.1 lentivirus vector (Addgene plasmid # 24150) for ERBB4 or SMAD4 knockdown. shRNA sequences were as follows:

shERBB4-1: 5'-CAGAGATGCAATGATAAGTTAT-3';
 shERBB4-2: 5'-AGAGTTGGTGGAACCATTAAC-3';
 shSMAD4: 5'-CAGATTGTCTTGCAACTTCAG-3'.

Quantitative reverse-transcription PCR (RT-qPCR)

Total RNAs were isolated from cells using TRIzol Reagent (Sigma), and 500 ng of total RNAs were reverse-transcribed into cDNA using PrimeScript RT Master Mix (TaKaRa). cDNA was then diluted and used for real-time PCR by using Power SYBR Green PCR Master Mix (ThermoFisher Scientific) and the 7300 real-time PCR system (Applied Biosystems). RT-qPCR primers used in this study can be found in Table S1.

Generation of SMAD4 or ERBB4 knockout cells

A guide DNA sequence targeting *SMAD4* or *ERBB4* gene was cloned into lenti-CRISPRv2 vector (no. 52961, Addgene), and lentivirus was produced in HEK293T cells for A549 cell infection. The infected cells were selected with 1 µg/mL puromycin and diluted into 96-well plates to produce single cell clones. The cell colonies were picked up and genotyped by sequencing to confirm the successful gene editing.

The sequences of sgDNAs were as follows:

SMAD4 sgRNA: 5'-ATGTGATCTATGCCGTCTC-3'; ERBB4 sgRNA #1: 5'-TCTACAGTTCCAGTCCCTGA-3'; ERBB4 sgRNA #2: 5'-TGTGTGCAGAACAAATGTGA-3'; ERBB4 sgRNA #3: 5'-TAATGCGTAAATTCTCCAG-3'.

Immunoprecipitation and western blotting analysis

Immunoprecipitation and western blotting analysis were carried out as described previously.^{43,44} Briefly, cells were collected in lysis buffer (25 mM Tris-HCl [pH 7.5], 150 mM NaCl, 0.5% NP-40; protease and phosphatase inhibitors added before use), and cell lysates were cleared by centrifugation. The supernatants were used for immunoprecipitation with protein A Sepharose beads (G&E Healthcare) and a primary antibody. Precipitated proteins as well as the initial whole cell lysates were separated by SDS-PAGE, transferred onto PVDF membranes, incubated with primary and secondary antibodies, and detected with an enhanced chemiluminescence staining kit.

GST pulldown assay

Recombinant GST-SMAD4 proteins were purified from *E. coli* BL21 (DE3) strain, while FLAG tagged GFP and 4ICD proteins were produced by using an *in vitro* Transcription/Translation System (Promega). GST pulldown experiments were carried out as previously described.^{45,46}

In vitro phosphorylation assay

Briefly, 1 µg GST-SMAD4 protein was incubated with *in vitro* translated FLAG-ERBB4 and FLAG-ERBB4 (KM) in a 50 µL kinase reaction buffer (50 mM Tris-HCl (pH 7.5), 5 mM MgCl₂, 30 µM ATP) at 37°C for 0.5 h. Phosphorylation of SMAD4 was analyzed by western blotting with P-Tyr-100 antibody.

Luciferase reporter assay

Cell culture, transfection, and reporter assays were carried out as previously described.^{44,45} The reporter expression plasmids used in this study were SMAD3/SMAD4-dependent SBE-Luc⁴⁰ and CAGA-Luc.⁴¹ Briefly, 24 h after transfection, cells were treated with TGF-β (2 ng/mL) for 8 h, and the cell lysates were analyzed using the Dual Luciferase Reporter Assay kit (Promega). All assays were performed in triplicates, and all values were normalized for transfection efficiency against Renilla luciferase activities.

Immunofluorescence

Cells were cultured and treated on coverslips in 24-well plates. They were sequentially incubated with 4% formaldehyde, 0.3% Triton X-100, 5% BSA in PBS, primary antibodies, Alexa Fluor 546- or Alexa Fluor 488-conjugated secondary antibodies (Invitrogen) and DAPI. Images were collected with a Zeiss LSM880 confocal microscope (Carl Zeiss).

Nuclear and cytosolic fractionation

Cells were lysed in cytoplasmic lysis buffer (10 mM HEPES pH 7.5, 1.5 mM MgCl₂, 10 mM KCl, 5 mM EDTA, 0.5 mM DTT, 0.2% NP-40) for 15 min on ice. Nuclei were sedimented by centrifugation and the supernatant containing the cytoplasmic fraction removed. The nuclei were then washed in cytoplasmic lysis buffer and lysed in RIPA buffer (50 mM Tris-HCl pH 7.4, 150 mM NaCl, 0.25% SDS, 1% NP-40, and 1 mM EDTA) for 30 min on ice. Cell lysates were centrifuged and the supernatants were collected as the nuclear fraction.

GAL4 transactivation assay

GAL4 transactivation assay, and plasmids GAL4-SMAD4C or GAL4-DB were previously described.³¹ Briefly, plasmids encoding GAL4-SMAD4C or GAL4-DB were co-transfected with GAL4-luciferase plasmid pFR-Luc (Stratagene) and other expression plasmids into cells, and 24 h after transfection, the cells were treated with or without 2 ng/mL TGF-β for 8 h. The ability of the SMAD4 to transactivate the heterologous GAL4 promoter was quantitated by measuring luciferase expression from the GAL4 promoter.

Mass spectrometry analysis

SFB-SMAD4 and HA-ERBB4 were overexpressed in HEK293T cells by transfection and purified by streptavidin beads (GE Healthcare Life Sciences). They were then separated by SDS-PAGE gel and stained with Coomassie Brilliant Blue. SFB-SMAD4 band was cut out from the gel and digested with Glu-c protease and trypsin, followed by LC-MS/MS analysis. The detailed phosphorylation sites searching was described previously.³³

DNA pulldown assay

DNA pulldown using biotinylated SBE oligonucleotides was carried out as previously described.⁴⁵ Briefly, A549 or H1299 cells were collected in a DNA binding buffer (10 mM HEPES [pH 7.5], 150 mM NaCl, 1 mM MgCl₂, 0.5 mM EDTA, 0.5 mM dithiothreitol, 10% glycerol and 0.1% NP-40) with protease and phosphatase inhibitors, and the cell lysates were incubated with 50 nM biotinylated SBE oligonucleotides at 37°C for 30 min. DNA-bound proteins were precipitated with streptavidin beads (GE Healthcare Life Sciences) for 15 min, washed thoroughly with the DNA binding buffer, and examined by western blotting analysis.

ChIP assay

Briefly, cells were treated with TGF-β (2 ng/mL) for 8 h and, after extensive washing, were crosslinked with 1% formaldehyde at room temperature for 10 min. ChIP assay was performed using a ChIP Assay Kit (Pierce) as described previously.⁴⁵ The sequences of ChIP primers can be found in [Table S1](#).

Wound healing assay

Briefly, cells were seeded in 6-well plates, and a scratch was created using a sterile pipette tip and washed with PBS. The cells were then fed with fresh medium containing 2% FBS and TGF-β (2 ng/mL). Images were acquired (0 h) and at 24 h or 48 h of culture for wound closure measurement. The wound healing rate was approximated by this equation: (W₀-W₄₈)/W₀, where W₀ and W₄₈ represent the gap width at 0 h and 24/48 h, respectively, and the rate was statistically analyzed.

Transwell migration assay

Briefly, 6×10⁴ cells in 100 μL culture medium containing 2% FBS were seeded in the upper chamber (8-μm pore size; Corning Incorporated, USA) of transwell, while 600 μL culture medium containing 10% FBS and 2 ng/mL TGF-β were added to the lower well. After incubation for 24 h, cells in the upper side of the inserts were removed with a cotton swab. Migrated cells of the lower side of the inserts were fixed in 4% PFA, stained with 0.5% crystal violet, and photographed. Migrated cells were counted from three random fields, quantitated by ImageJ and statistically analyzed.

Cell proliferation and cell cycle assays

Cells were seeded in a 24-well plate at a density of 0.4×10⁵ cells/well and cultured in the absence or presence of TGF-β (2 ng/mL) for 48 h. Cell proliferation (DNA synthesis) was detected by Click-iT EdU Kit. EdU (5-ethynyl 20-deoxyuridine)- positive cells were counted under a microscope.

For cell cycle analysis, 1×10⁶ cells (with or without 2 ng/mL TGF-β treatment for 48 h) were collected, washed with ice-cold PBS, fixed by 70% ethanol, and re-suspended in 1 mL of PBS containing RNase A and 0.1 mg/mL propidium iodide before subjected to analysis by Flow Cytometer. The results of fluorescence measurements were displayed as cellular DNA content frequency histograms. The proportions of cells in the respective phases of the cycle were analyzed and calculated.

Mouse tumor model

Seven-week-old female NOD SCID mice were used in this study. To generate mouse tumor model, 2×10⁶ luciferase-expressing A549 cells (in 200 μL PBS) were injected into mice ($n = 6/\text{group}$) through the lateral tail vein. Bioluminescence imaging of tumor metastasis was carried out 2 months after cell injection. Then, all animals were euthanized, and the lungs were dissected and fixed in 4% paraformaldehyde. Metastatic foci were quantitated by visual inspection, and haematoxylin and eosin (H&E) staining were performed on the lung sections. All mice were maintained in pathogen-free facilities at Zhejiang University. All animal experiments were approved by Zhejiang University Committee for Experimental Animal Studies and Ethics (No. 16896) and performed in accordance with the ethical regulations regarding animal research.

IHC analysis

The tissue sections from paraffin-embedded mice lung tumors were deparaffinized with xylene and rehydrated with an alcohol gradient and water. Sections were incubated with primary antibodies (anti-SMAD4 PY162 or ERBB4) at room temperature for 1 h and biotin-labelled secondary antibodies for 1 h, and then stained with peroxidase streptavidin (Jackson ImmunoResearch) and DAB peroxidase substrate kit (Solarbio LIFE SCIENCES).

QUANTIFICATION AND STATISTICAL ANALYSIS

Data were presented as mean ± standard error of mean (SEM) from at least three biologically independent samples. When appropriate, statistical differences between multiple comparisons were analyzed using the two-tailed Student's t-test. The representative data shown in the figures were repeated at least three times independently. Western blotting, immunofluorescence staining, as well as mouse tumor assays were performed three times independently, and similar results were obtained.